Rotordynamic Analyses using Finite Element Method

A Thesis
Presented to
the faculty of the School of Engineering and Applied Science
University of Virginia

In Partial Fulfillment
of the requirements for the Degree
Master of Science

By:
Michael Branagan
May 2014

APPROVAL SHEET

The Thesis
is submitted in partial fulfillment of the requirements
for the degree of
Master of Science

AUTHOR

The thesis has been read and approved by the examining committee:

Houston G. Wood, III
Advisor

Robert Durgin Rockwell, Jr
Advisor

Richard Wesley Kent

Accepted for the School of Engineering and Applied Science:

Dean, School of Engineering and Applied Science

May

2014

Abstract

The ability to perform critical frequency and forced response analyses is a vital tool for designing and troubleshooting rotordynamic systems. These analyses can be a challenge due to the wide variety of components found in rotordynamic systems. There are a variety of methods that can be used to perform these analyses. The finite element method is one method that can be used to perform these analyses.

A finite element approach to rotordynamic analyses is presented in this thesis. First, the finite element model is developed. The equations of motion that are used to analyze the finite element model are developed. Next the development of a MATLAB based rotordynamic tool incorporating this method is presented. The features of this tool, including degree-of-freedom coupling, multiple rotor systems, and the inclusion of tilting pad bearings with full coefficients, aerodynamic cross couplings, thrust bearings, flexible bearing supports, flexible couplings, and the stiffness properties of disks in the model, are presented as well as improvements that have been made to the efficiency of the program. Finally program is verified by comparison to a case study for both stability and forced response analyses and validated with a different case study. The verification case is a classic eight stage compressor rotor model that has been widely used as a test case for other industry software. The validation case study is a ROMAC test rig used to study stability. In both cases, differences of less than 5% were found. These cases illustrate the accuracy of the methods developed in this thesis.

Table of Contents

List of Figures

List of Tables

Nomenclature

α	Axial tensile force
$[C]$	Gyroscopic matrix
$\{F\}$	Force vector
$\{F\}$	Torque vector
$\{F\}$	Unbalance Force Magnitude Vector
$\{g\}$	Axial force
$[G]$	Damping matrix
$[K]$	Stiffness matrix
$[M]$	Mass matrix
$[R]$	Generalized Rotor Matrix
$\{U\}$	Displacement Magnitude Vector
$\{V\}$	State Space Magnitude Vector
$\{v\}$	State Space Vector
$\{w\}, \{q\}$	Displacement vector
κ	Shape factor
Ω	Rotating speed
Φ	Shear Effect Parameter
ϕ	Diameter

Ψ	Translation displacement function
ρ	Density
τ	Applied external moment
θ_x	Rotation angle about the x-axis
θ_y	Rotation angle about the y-axis
θ_z	Rotation angle about the z-axis
Υ	Internal torque
ϖ, z	Displacement along the z-axis
ς	Cross Coupling Magnitude
Ξ	Generalized forces
ξ	Rotational displacement function
ζ	Generalized coordinates
A	Cross Sectional Area
E	Young's Modulus
f	Applied external force
G	Shear modulus
g	Axial force
I_d	Diametrical area moment of inertia
I_p	Polar area moment of inertia
k	stiffness
L	Length
M	Internal bending moment
m	Mass
N	Shape functions
Q	Shear force

r	Generalized Rotor Matrix Element
s	Position along the z-axis
T	Kinetic energy
u, x	Displacement along the x-axis
V	Potential energy
v, y	Displacement along the y-axis

1 Introduction

1.1 Rotordynamics

Rotordynamics is a specialized branch of applied mechanics dealing with the behavior of rotating objects, known as rotors. Rotors can be found in machinery applications such as:

- Jet Engines
- Power Generation
- Medical Applications
- Machining Tools
- Turbomachinery
- Motors

An understanding of rotordynamics has increasing importance as rotating machines are required to operate at ever increasing speeds and in more and more challenging environments.

"On The Centrifugal Force of Rotating Shafts"[1] written by Rankine in 1869 is commonly accepted as the first paper written solely on the subject of rotordynamics. In it the author determines that rotors will experience large amplitude vibrations at certain running speeds, called critical speeds. However, he incorrectly stated that it was impossible to run the machine faster than the critical speed without experiencing machine failure.

In 1895, the works of Dunkerley[2] and F$\ddot{o}$ppel[3] improved the understanding of operating speeds greater than the first critical speed. It was discovered that rotors have multiple critical speeds and that some of them correspond to the natural frequencies of a non-rotating shaft. In 1919, Jeffcott[4] helped improve this understanding using a lumped parameter approach. The Jeffcott rotor is a useful but very simple rotor model. Today's highly complex rotors running at increasingly fast speeds in varied environments require more sophisticated methods in order to understand their motion. With the development of computers there have been new computational techniques that allow for more complex and accurate analyses. Transfer matrix method and finite element method are two such techniques. This thesis focuses on the finite element approach.

1.2 Finite Element Method

Many phenomena in engineering can be described using partial differential equations. Solving these equations using analytical methods can be close to impossible for arbitrary shapes. The finite element method is a numerical method for getting approximate solutions to these partial differential equations.

In order to execute the finite element method, the model must be discretized into a series of subdomains called elements. These elements are defined and connected by several points known as nodes. The process by which the model is discretized into elements and nodes is called meshing. The partial differential equation that describes the physical phenomena can then be approximated with a series of ordinary differential equations.

The finite element method has been developed and validated for use with rotordynamic systems. In 1970, Ruhl[6] was one of the first to study the finite element method as it is applied to rotordynamics. His finite element approach included translational inertia and bending stiffness, but neglected rotary inertia, gyroscopic moments, and shear deformation. Around the same time, Thorkildsen[7] developed a finite element model that was similar to Rhul's model but included rotary inertia and gyroscopic moments. In 1974, Polk[8] developed a finite element rotor model using Timoshenko beam theory. However, he did not present any actual numbers with this model. In 1980, Nelson[9] presented numerical studies for the elements developed by Polk.

1.3 ROMAC Rotordynamic Codes

The Rotating Machinery and Controls (ROMAC) lab at the University of Virginia strives to advance the field of rotordynamics for the benefit of its industrial partners. ROMAC performs both theoretical and experimental research in the general areas of rotordynamics, magnetic bearings, tilting pad bearings, seals, squeeze film dampers, turbomachinery, and structural dynamics.[10]

ROMAC has been working in the field of rotordynamics since 1972. This includes a rich history of numerical analysis software development for use in the field of rotordynamics, which are available to their members. This history includes the development of analytical and computational methods, software implementations, and perhaps most importantly experience in correlating experimental and field test data with model analyses for the ongoing process of continuously improving the analysis techniques.[11]

Some of the current ROMAC codes are:

- ROTSTB

  ROTSTB uses the transfer matrix method in order to analyze the lateral stability of the rotor. It allows separate mass and stiffness diameters for the shaft.

- CRTSP2

  CRTSP2 is used to produce a critical speed map for the lateral degrees of freedom. This is a powerful tool in the early stages of rotordynamic design. It uses the transfer matrix method and is capable of finding the free-free modes.

- FORSTAB

  FORSTAB uses the finite element method to perform lateral forced response analysis and stability analysis. It uses a modal representation of the rotor models and is limited to lateral degrees of freedom.

- TWIST2

  TWIST2 is a torsional vibration analysis code that can perform stability analysis and steady state forced response analysis using the finite element method.

1.4 RotorSol

RotorSol (previously known as MatlabRotor) was developed as a finite element steady-state solver that couples lateral, torsional, and axial degrees of freedom together. It was developed initially by Chaudry[11] using twelve-degree-of-freedom beam elements that incorporate the lateral, torsional, and axial degrees of freedom. The rotor models were analyzed using either a stability analysis or a forced response analysis in the lateral or fully coupled directions. The rotor models could include the following possible components: shaft with constant diameter sections, lumped masses, solid geometry bearings (or the synchronously reduced coefficients of tilting pad bearings), probes, and mass unbalances. Matlab was used as the programming platform in order to take advantage of the mathematical and graphical tools developed and maintained by MathWorks[12].

This thesis extends the capabilities of RotorSol in several ways. First, RotorSol is now capable of performing any coupling combination of the lateral, torsional, and axial directions. This allows for the inclusion of such components as gears, flexible couplings, thrust bearings with the ability to

find any possible mixed mode that results. These mixed modes are commonly found in systems with gearboxes. Kaplan illustrated one example of this in his Masters thesis[13].

RotorSol is also now capable of analyzing systems which contain any number of rotors. This is important due to the dynamic interaction between the rotors found in high speed multi-rotor systems such as jet engines. This thesis will develop the inclusion of components such as tilting pad bearings with full coefficients, aerodynamic cross couplings, thrust bearings, flexible couplings and flexible support for the bearings into the rotor model. These new features allow many more real rotordynamic systems to be modeled and analyzed. RotorSol is now capable of outputting the system matrices to allow the user to make changes or export to other programs for analyses not directly performed in RotorSol itself.

1.5 Thesis Outline

In Chapter 2, the governing equations for a rotor are developed. They are developed separately for the lateral, torsional, and axial degrees of freedom. Next, the finite element method is examined as a means of solving the governing rotordynamic equations. The developed rotor and component matrices are presented. Lastly, the full set of equations of motions that are used in RotorSol are presented. Chapter 3 presents RotorSol as a solution for solving rotordynamic problems using the finite element method. The various features of RotorSol are presented. There is also a discussion of several improvements in efficiency that have been implemented in RotorSol as part of the current work. Chapter 4 presents verification and validation results for RotorSo with comparisons to other ROMAC codes as well as experimental results.

2 Theory

This chapter develops the finite element equations for rotordynamic systems using Lagrange's equation and twelve degree-of-freedom beam elements. First the coninuous model and the lumped parameter model for each direction (lateral, axial and torsional) will be presented. Then the lumped parameter models will be used to create the finite element equations for the rotor. Then the contribution for each component is presented. Lastly the solution method for the equations of motion are presented.

The equations of motion for rotordynamic systems are developed by applying dynamic principles to appropriate models. The models can be represented as continuous models which result in partial differential equations or lumped parameter models which result in matrix equations.

2.1 Lateral Degrees of Freedom

2.1.1 Continuous Model

A continuous rotor model is illustrated in Figure 1. Consider an axial dif-

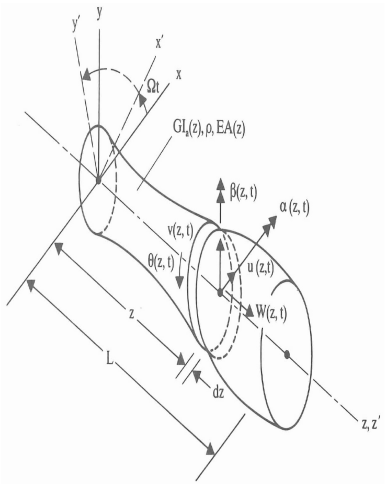

Figure 1: Continuous Rotor Model[14]

ferential element of length dz. Let ρA be the mass per unit length, ρI_d be the diametrical moment of inertia per unit length, and ρI_p be the axial moment of inertia per unit length. Let the lateral motions of the differential element be defined by displacements $u(z,t)$ and $v(z,t)$ and angular displacements of $\theta_x(z,t)$ and $\theta_y(z,t)$. Then the internal bending moments transmitted by the differential element at z are

$$M_x = EI_d \frac{\partial \theta_y}{\partial z} \tag{2.1}$$

$$M_y = EI_d \frac{\partial \theta_x}{\partial z} \tag{2.2}$$

and the shear forces are

$$Q_x = \kappa GA(\frac{\partial u}{\partial z} - \theta_x) \tag{2.3}$$

$$Q_y = \kappa GA(\frac{\partial v}{\partial z} + \theta_y). \tag{2.4}$$

The bending modulus , EI_d, effective shear modulus, κGA, and inertia properties are dependent upon the axial position z along the rotor.

Let forces $f_x(z,t)$ and $f_y(z,t)$ and torques $\tau_x(z,t)$ and $\tau_y(z,t)$ are applied to the rotor per unit length. Assuming the rotor is spinning at a constant rate of Ω, then the following four partial differential equations[14] can be obtained.

$$\rho A \frac{\partial^2 u}{\partial t^2} - \frac{\partial}{\partial z}[\kappa GA(\frac{\partial u}{\partial z} - \theta_x)] = f_x \tag{2.5}$$

$$\rho A \frac{\partial^2 v}{\partial t^2} - \frac{\partial}{\partial z}[\kappa GA(\frac{\partial v}{\partial z} - \theta_y)] = f_y \tag{2.6}$$

$$\rho I_d \frac{\partial^2 \theta_y}{\partial t^2} + \Omega \rho I_p \frac{\partial \theta_x}{\partial t} - \frac{\partial}{\partial z}(EI_d \frac{\partial \theta_y}{\partial z}) + \kappa GA(\frac{\partial v}{\partial z} + \theta_y) = \tau_x \tag{2.7}$$

$$\rho I_d \frac{\partial^2 \theta_x}{\partial t^2} - \Omega \rho I_p \frac{\partial \theta_y}{\partial t} - \frac{\partial}{\partial z}(EI_d \frac{\partial \theta_x}{\partial z}) - \kappa GA(\frac{\partial u}{\partial z} - \theta_x) = \tau_y \tag{2.8}$$

In order to finish the formulation of the partial differential equations, the values of the discplacements at the ends of the rotor are used along with Equations 2.1 - 2.4.

2.1.2 Lumped Parameter Model

Solving for the continuous rotor model can be a time intensive process. It is often less costly to use a lumped parameter model without much loss of accuracy. For lumped-parameter models, Lagrange's equation (Equation 2.9) can be used to solve for the equations of motion:

$$\frac{d}{dt}(\frac{\partial T}{\partial \dot{\zeta}_i}) - \frac{\partial T}{\partial \zeta_i} + \frac{\partial V}{\partial \zeta_i} = \Xi \tag{2.9}$$

where T is the global kinetic energy, V is the global potential energy, ζ_i are the generalized coordinates and Ξ are the generalized forces not included in V.

The kinetic energy[14] contains both translational and rotational components.

$$T = \frac{1}{2}\sum_{i=1}^{n}[m_i(\dot{x}^2 + \dot{y}^2) + I_{d_i}(\dot{\theta_x}^2 + \dot{\theta_y}^2) + \Omega I_{p_i}(\dot{\theta}_x\theta_y - \theta_x\dot{\theta_y}) + \Omega^2 I_{p_i}] \tag{2.10}$$

The potential energy[14] term consists of elastic bending energy due to the bending moments and shear energy due to the shear forces [11]. The total potential energy function is:

$$V = \frac{1}{2}\sum_{i=1}^{n}[EI_d(\frac{\partial\theta_x}{\partial z}^2 + \frac{\partial\theta_y}{\partial z}^2) + \kappa GA((\frac{\partial x}{\partial z} - \theta_y)^2 + (\frac{\partial y}{\partial z} + \theta_x)^2)]. \tag{2.11}$$

The only generalized force that is considered but is not included in the potential energy term is the force due to the mass unbalance of the rotor.

Using Langrange's equations (Equation 2.9) and Equations 2.10 - 2.11, the lateral equations of motion[14] for the rotor can be found:

$$\left[M\right]\left\{\ddot{w}\right\}_{lateral} + \dot{\phi}\left[G\right]\left\{\dot{w}\right\}_{lateral} + \left[K\right]\left\{w\right\}_{lateral} = \left\{F\right\}e^{i\Omega t} \tag{2.12}$$

where w is the displacement vector given by Equation 2.13, M is the mass matrix including both translational and rotational mass, G is the gyroscopic matrix, K is the stiffness matrix and F is the force vector due to the unbalance force.

$$\left\{w\right\}_{lateral} = \begin{Bmatrix} x(t) \\ y(t) \\ \theta_x(t) \\ \theta_y(t) \end{Bmatrix} \tag{2.13}$$

Assuming the angular velocity is constant, Equation 2.12 can be rewritten.

$$\left[M\right]\left\{\ddot{w}\right\}_{lateral} + \Omega\left[G\right]\left\{\dot{w}\right\}_{lateral} + \left[K\right]\left\{w\right\}_{lateral} = \left\{F\right\}e^{i\Omega t} \tag{2.14}$$

2.2 Torsional Degrees of Freedom

2.2.1 Continuous Model

Again consider the continuous Rotor Model in Figure 1. The torque transmitted across the differential element is

$$\Upsilon_z = GI_p \frac{\partial \theta_z}{\partial z}. \tag{2.15}$$

where GI_p varies along z. If an axial torque, $\tau_z(z,t)$, per unit length is applied to the rotor then the partial differential equation[14]

$$-\frac{\partial}{\partial z}(GI_p \frac{\partial \theta_z}{\partial z}) + \rho I_p \frac{\partial^2 \theta_z}{\partial t^2} = \tau_z \tag{2.16}$$

can be developed. Assuming external axial torques, τ_{z0} and τ_{zL} are applied at either end of the rotor, this partial differential equation along with the boundary conditions

$$-(GI_p \frac{\partial \theta_z}{\partial z})_0 = \tau_{z_0} \quad at\ z = 0 \tag{2.17}$$

and

$$-(GI_p \frac{\partial \theta_z}{\partial z})_L = \tau_{z_L} \quad at\ z = L \tag{2.18}$$

can be used to determine the torsional vibration of the rotor.

2.2.2 Lumped Parameter Model

Again this paper will develop the lumped parameter model for torsional vibration. Using Lagrange's equations (2.9),

$$T_{torsional} = \frac{1}{2} \sum_{i=1}^{n} I_{p_i} \dot{\theta_{z_i}}^2, \tag{2.19}$$

$$V_{torsional} = \frac{1}{2} \sum_{i=1}^{n-1} k_i (\theta_{z_{i+1}} - \theta_{z_i})^2, \tag{2.20}$$

and a generalized force, Ξ_i, of τ_{z_i} the torsional equations of motion[14] can be developed.

$$\left[M\right] \left\{\ddot{w}\right\}_{torsional} + \left[K\right] \left\{w\right\}_{torsional} = \left\{\tau\right\} \tag{2.21}$$

2.3 Axial Degrees of Freedom

2.3.1 Continuous Model

Using the discretized element found in Figure 1, the axial tensile force across the element is

$$\alpha = EA\frac{\partial \varpi}{\partial z} \tag{2.22}$$

where ϖ is the axial displacement. If an axial force g(z,t) is applied per unit length to the continuous rotor then one can derive Equation 2.23[14].

$$-\frac{\partial}{\partial z}(EA\frac{\partial \varpi}{\partial z}) + \rho A\frac{\partial^2 \varpi}{\partial t^2} = g \tag{2.23}$$

The boundary conditions are dependent upon the configuration of the rotor. For example, boundary conditions for a rotor constrained by a spring at one end and forces, $g_0(t)$ and $g_L(t)$ are

$$k_0\varpi(0,t) - (EA\frac{\partial \varpi}{\partial z})_0 = g_0(t) \tag{2.24}$$

$$(EA\frac{\partial \varpi}{\partial z})_L = g_L(t) \tag{2.25}$$

where k_0 is a spring stiffness of an axial spring connected to the $z = 0$ end of the rotor.

2.3.2 Lumped Parameter Model

Using Lagrange's equations (2.9),

$$T_{axial} = \frac{1}{2}\sum_{i=1}^{n} m_i\dot{\varpi_i}^2 \tag{2.26}$$

$$V_{axial} = \frac{1}{2}k_0\varpi_1^2 + \frac{1}{2}\sum_{i=1}^{n-1} k_i(\varpi_{i+1} - \varpi_i)^2, \tag{2.27}$$

and a generalized force, Ξ_i, of g_i the axial equations of motion[14] can be developed.

$$\left[M\right]\left\{\ddot{w}\right\}_{axial} + \left[K\right]\left\{w\right\}_{axial} = \left\{g\right\} \tag{2.28}$$

2.4 Beam Elements

In order to analyze the lateral, torsional and axial degrees of freedom, twelve degrees of freedom beam elements are used. Both nodes of these elements can translate in the lateral (x,y) and axial (z) directions and rotate in the lateral (θ_x, θ_y) and torsional (θ_z) directions. This type of element is illustrated below. These elements are used by taking each of the direc-

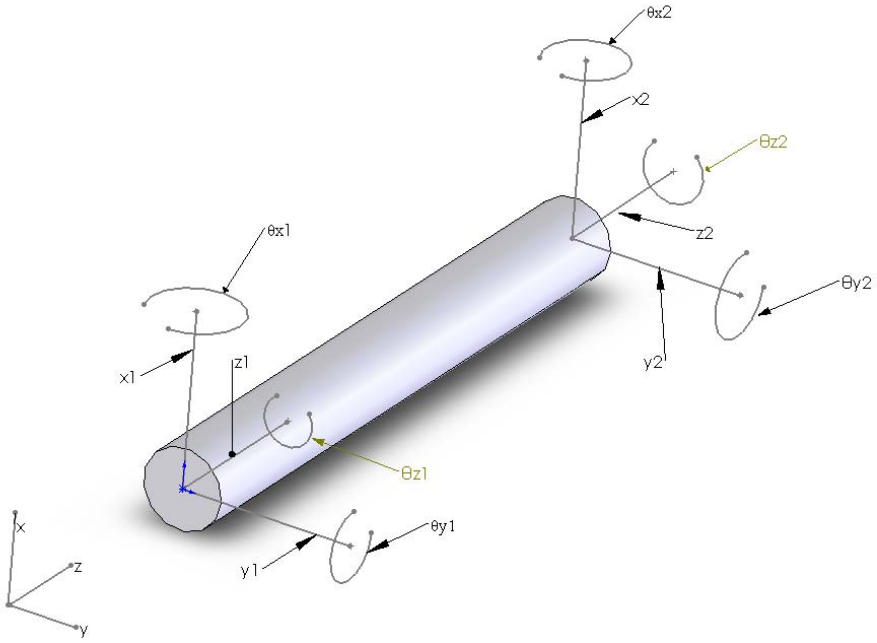

Figure 2: Twelve Degree of Freedom Beam Element [11]

tional lumped parameter models and developing the rotor elements. Then the elemental matrices are combined in order to form the full rotor matrices.

2.4.1 Lateral Elements

In order to form elements, shape functions are used to assume a shape for the displacements across the elements. For the lateral element, the translation and rotation of a point along the element can be approximated as:

$$\begin{Bmatrix} x(s,t) \\ y(s,t) \\ \theta_x(s,t) \\ \theta_y(s,t) \end{Bmatrix} = \begin{bmatrix} \Psi_1 & 0 & 0 & \Psi_2 & \Psi_3 & 0 & 0 & \Psi_4 \\ 0 & \Psi_1 & \Psi_2 & 0 & 0 & \Psi_3 & \Psi_4 & 0 \\ 0 & \xi_1 & \xi_2 & 0 & 0 & \xi_3 & \xi_4 & 0 \\ \xi_1 & 0 & 0 & \xi_2 & \xi_3 & 0 & 0 & \xi_4 \end{bmatrix} \{q(t)\} \tag{2.29}$$

where the individual shape functions, $\Psi_i(s) = \frac{1}{1+\Phi}[\eta_i(s)+\Phi\lambda_i(s)]$ and $\xi_i(s) = \frac{1}{1+\Phi}[\epsilon_i(s) + \Phi\delta_i(s)], i = 1, 2, 3, 4$, represent static displacement and rotation shape functions associated with unit displacements of one of the endpoint coordinates with all other coordinates constrained to zero [9].

2.4.2 Torsional Elements

A torsional element consists of one degree of freedom at each node, θ_z. The angular displacement can be defined as:

$$\theta_z^{(e)}(z) = N_i^{(e)}\theta_{zi} + N_j^{(e)}\theta_{zj} \ , \ 0 \leq z' \leq L \tag{2.30}$$

where the $N_i^{(e)}$ and $N_j^{(e)}$ are linear shape functions for an element with node i and j.

$$\left[N\right]_t^{(e)} = \left[N_i \quad N_j\right]^{(e)} = \left[1 - \tfrac{z'}{L} \quad \tfrac{z'}{L}\right] \tag{2.31}$$

and

$$z' = z - z_i. \tag{2.32}$$

These shape functions are shown in Figure 3 and Figure 4. The elemental angular displacement is shown in Figure 5.

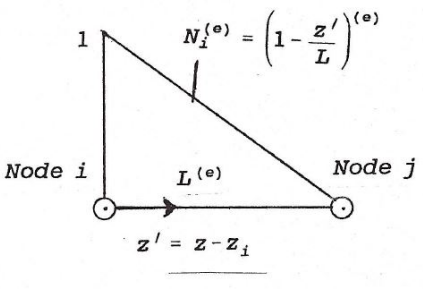

Figure 3: Linear Shape Function for Node i [15]

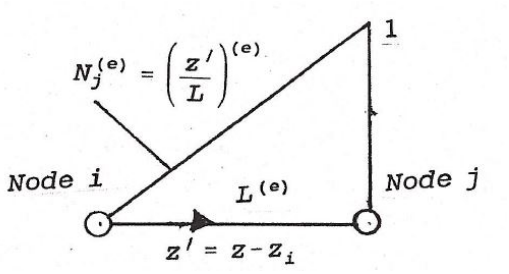

Figure 4: Linear Shape Function for Node j [15]

2.4.3 Axial Elements

The axial element has two degrees of freedom. The axial displacement across the element can be approximated by using the same linear shape functions as those used for the torsional elements.

$$\varpi^{(e)}(z) = N_i^{e)}\varpi_i + N_j^{(e)}\varpi_j \ , \ 0 \leq z' \leq L^{(e)} \tag{2.33}$$

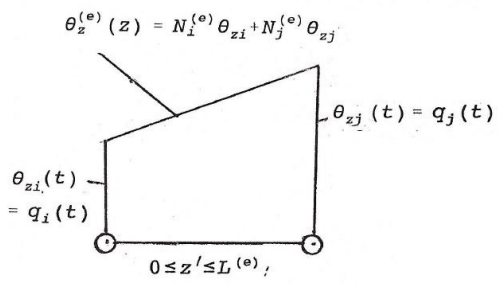

Figure 5: Angular Displacement Across Element e [15]

2.5 Rotor Matrices

These elements have mass, stiffness, damping and gyroscopic matrices that are derived separately in Sections 2.1.2, 2.2.2, and 2.3.2 in the lateral, axial and torsional directions. The separate matrices are combined to form the full twelve degree of freedom rotor matrices. This done by assembling the matrices as follows.

$$[R]^{(e)} = \begin{bmatrix}
r_{z_1z_1} & 0 & 0 & 0 & 0 & 0 & r_{z_1z_2} & 0 & 0 & 0 & 0 & 0 \\
0 & r_{x_1x_1} & r_{x_1y_1} & 0 & r_{x_1\theta_{x1}} & r_{x_1\theta_{y1}} & 0 & r_{x_1x_2} & r_{x_1y_2} & 0 & r_{x_1\theta_{x2}} & r_{x_1\theta_{y2}} \\
0 & r_{y_1x_1} & r_{y_1y_1} & 0 & r_{y_1\theta_{x1}} & r_{y_1\theta_{y1}} & 0 & r_{y_1x_2} & r_{y_1y_2} & 0 & r_{y_1\theta_{x2}} & r_{y_1\theta_{y2}} \\
0 & 0 & 0 & r_{\theta_{z1}\theta_{z1}} & 0 & 0 & 0 & 0 & 0 & r_{\theta_{z1}\theta_{z2}} & 0 & 0 \\
0 & r_{\theta_{x1}x_1} & r_{\theta_{x1}y_1} & 0 & r_{\theta_{x1}\theta_{x1}} & r_{\theta_{x1}\theta_{y1}} & 0 & r_{\theta_{x1}x_2} & r_{\theta_{x1}y_2} & 0 & r_{\theta_{x1}\theta_{x2}} & r_{\theta_{x1}\theta_{y2}} \\
0 & r_{\theta_{y1}x_1} & r_{\theta_{y1}y_1} & 0 & r_{\theta_{y1}\theta_{x1}} & r_{\theta_{y1}\theta_{y1}} & 0 & r_{\theta_{y1}x_2} & r_{\theta_{y1}y_2} & 0 & r_{\theta_{y1}\theta_{x2}} & r_{\theta_{y1}\theta_{y2}} \\
r_{z_2z_1} & 0 & 0 & 0 & 0 & 0 & r_{z_2z_2} & 0 & 0 & 0 & 0 & 0 \\
0 & r_{x_2x_1} & r_{x_2y_1} & 0 & r_{x_2\theta_{x1}} & r_{x_2\theta_{y1}} & 0 & r_{x_2x_2} & r_{x_2y_2} & 0 & r_{x_2\theta_{x2}} & r_{x_2\theta_{y2}} \\
0 & r_{y_2x_1} & r_{y_2y_1} & 0 & r_{y_2\theta_{x1}} & r_{y_2\theta_{y1}} & 0 & r_{y_2x_2} & r_{y_2y_2} & 0 & r_{y_2\theta_{x2}} & r_{y_2\theta_{y2}} \\
0 & 0 & 0 & r_{\theta_{z2}\theta_{z1}} & 0 & 0 & 0 & 0 & 0 & r_{\theta_{z2}\theta_{z2}} & 0 & 0 \\
0 & r_{\theta_{x2}x_1} & r_{\theta_{x2}y_1} & 0 & r_{\theta_{x2}\theta_{x1}} & r_{\theta_{x2}\theta_{y1}} & 0 & r_{\theta_{x2}x_2} & r_{\theta_{x2}y_2} & 0 & r_{\theta_{x2}\theta_{x2}} & r_{\theta_{x2}\theta_{y2}} \\
0 & r_{\theta_{y2}x_1} & r_{\theta_{y2}y_1} & 0 & r_{\theta_{y2}\theta_{x1}} & r_{\theta_{y2}\theta_{y1}} & 0 & r_{\theta_{y2}x_2} & r_{\theta_{y2}y_2} & 0 & r_{\theta_{y2}\theta_{x2}} & r_{\theta_{y2}\theta_{y2}}
\end{bmatrix}$$

where R is just a general system matrix.

The system matrices for the rotor are:

Element Mass Matrix:

$$[M]^{(e)} = \rho AL \begin{bmatrix}
\frac{1}{3} & 0 & 0 & 0 & 0 & 0 & \frac{1}{6} & 0 & 0 & 0 & 0 & 0 \\
0 & frA & 0 & 0 & 0 & frC & 0 & frB & 0 & 0 & 0 & -frD \\
0 & 0 & frA & 0 & -frC & 0 & 0 & 0 & frB & 0 & frD & 0 \\
0 & 0 & 0 & \frac{2I_d}{3A} & 0 & 0 & 0 & 0 & 0 & \frac{2I_d}{6A} & 0 & 0 \\
0 & 0 & -frC & 0 & frE & 0 & 0 & 0 & -frD & 0 & frF & 0 \\
0 & frC & 0 & 0 & 0 & frE & 0 & frD & 0 & 0 & 0 & frF \\
\frac{1}{6} & 0 & 0 & 0 & 0 & 0 & \frac{1}{3} & 0 & 0 & 0 & 0 & 0 \\
0 & frB & 0 & 0 & 0 & frD & 0 & frA & 0 & 0 & 0 & -frC \\
0 & 0 & frB & 0 & -frD & 0 & 0 & 0 & frA & 0 & frC & 0 \\
0 & 0 & 0 & \frac{2I_d}{6A} & 0 & 0 & 0 & 0 & 0 & \frac{2I_d}{3A} & 0 & 0 \\
0 & 0 & frD & 0 & frF & 0 & 0 & 0 & frC & 0 & frE & 0 \\
0 & -frD & 0 & 0 & 0 & frF & 0 & -frC & 0 & 0 & 0 & frE
\end{bmatrix}$$

where

$$frA = \frac{\frac{13}{35} + \frac{7}{10}\Phi + \frac{1}{3}\Phi^2 + \frac{6I_d}{5AL^2}}{(1+\Phi)^2}$$

$$frB = \frac{\frac{9}{70} + \frac{3}{10}\Phi + \frac{1}{6}\Phi^2 - \frac{6I_d}{5AL^2}}{(1+\Phi)^2}$$

$$frC = \frac{(\frac{11}{210} + \frac{11}{120}\Phi + \frac{1}{24}\Phi^2 + (\frac{1}{10} - \frac{\Phi}{2})\frac{I_d}{AL^2})L}{(1+\Phi)^2}$$

$$frD = \frac{(\frac{13}{420} + \frac{3}{40}\Phi + \frac{1}{24}\Phi^2 - (\frac{1}{10} - \frac{\Phi}{2})\frac{I_d}{AL^2})L}{(1+\Phi)^2}$$

$$frE = \frac{(\frac{1}{105} + \frac{1}{60}\Phi + \frac{1}{120}\Phi^2 + (\frac{2}{15} + \frac{\Phi}{6} + \frac{\Phi^2}{3})\frac{I_d}{AL^2})L^2}{(1+\Phi)^2}$$

$$frF = \frac{(-\frac{1}{140} - \frac{1}{60}\Phi - \frac{1}{120}\Phi^2 + (-\frac{1}{30} - \frac{\Phi}{6} + \frac{\Phi^2}{6})\frac{I_d}{AL^2})L^2}{(1+\Phi)^2}.$$

Element Stiffness Matrix:

$$[K]^{(e)} = \frac{EI_d}{(1+\Phi)L^3}\begin{bmatrix}
\frac{AE}{L*Const} & 0 & 0 & 0 & 0 & 0 & -\frac{AE}{L*Const} & 0 & 0 & 0 & 0 & 0 \\
0 & 12 & 0 & 0 & 0 & 6L & 0 & -12 & 0 & 0 & 0 & 6L \\
0 & 0 & 12 & 0 & -6L & 0 & 0 & 0 & -12 & 0 & -6L & 0 \\
0 & 0 & 0 & \frac{2GI_d}{L*Const} & 0 & 0 & 0 & 0 & 0 & -\frac{2GI_d}{L*Const} & 0 & 0 \\
0 & 0 & -6L & 0 & (4+\Phi)L^2 & 0 & 0 & 0 & 6L & 0 & (2-\Phi)L^2 & 0 \\
0 & 6L & 0 & 0 & 0 & (4+\Phi)L^2 & 0 & -6L & 0 & 0 & 0 & (2-\Phi)L^2 \\
-\frac{AE}{L*Const} & 0 & 0 & 0 & 0 & 0 & \frac{AE}{L*Const} & 0 & 0 & 0 & 0 & 0 \\
0 & -12 & 0 & 0 & 0 & -6L & 0 & 12 & 0 & 0 & 0 & -6L \\
0 & 0 & -12 & 0 & 6L & 0 & 0 & 0 & 12 & 0 & 6L & 0 \\
0 & 0 & 0 & -\frac{2GI_d}{L*Const} & 0 & 0 & 0 & 0 & 0 & \frac{2GI_d}{L*Const} & 0 & 0 \\
0 & 0 & -6L & 0 & (2-\Phi)L^2 & 0 & 0 & 0 & 6L & 0 & (4+\Phi)L^2 & 0 \\
0 & 6L & 0 & 0 & 0 & (2-\Phi)L^2 & 0 & -6L & 0 & 0 & 0 & (4+\Phi)L^2
\end{bmatrix}$$

where

$$Const = \frac{EI_d}{(1+\Phi)L^3}.$$

Element Gyroscopic Matrix:

$$[G]^{(e)} = 2\rho AL\begin{bmatrix}
0 & 0 & 0 & 0 & 0 & 0 & 0 & 0 & 0 & 0 & 0 & 0 \\
0 & 0 & f\bar{r}A & 0 & f\bar{r}B & 0 & 0 & 0 & -f\bar{r}A & 0 & f\bar{r}B & 0 \\
0 & -f\bar{r}A & 0 & 0 & 0 & f\bar{r}B & 0 & f\bar{r}A & 0 & 0 & 0 & f\bar{r}B \\
0 & 0 & 0 & 0 & 0 & 0 & 0 & 0 & 0 & 0 & 0 & 0 \\
0 & -f\bar{r}B & 0 & 0 & 0 & f\bar{r}C & 0 & f\bar{r}B & 0 & 0 & 0 & f\bar{r}D \\
0 & 0 & -f\bar{r}B & 0 & -f\bar{r}C & 0 & 0 & 0 & f\bar{r}B & 0 & f\bar{r}D & 0 \\
0 & 0 & 0 & 0 & 0 & 0 & 0 & 0 & 0 & 0 & 0 & 0 \\
0 & 0 & -f\bar{r}A & 0 & -f\bar{r}B & 0 & 0 & 0 & f\bar{r}A & 0 & -f\bar{r}B & 0 \\
0 & f\bar{r}A & 0 & 0 & 0 & -f\bar{r}B & 0 & -f\bar{r}A & 0 & 0 & 0 & -f\bar{r}B \\
0 & 0 & 0 & 0 & 0 & 0 & 0 & 0 & 0 & 0 & 0 & 0 \\
0 & -f\bar{r}B & 0 & 0 & 0 & -f\bar{r}D & 0 & f\bar{r}B & 0 & 0 & 0 & f\bar{r}C \\
0 & 0 & -f\bar{r}B & 0 & -f\bar{r}D & 0 & 0 & 0 & f\bar{r}B & 0 & -f\bar{r}C & 0
\end{bmatrix}$$

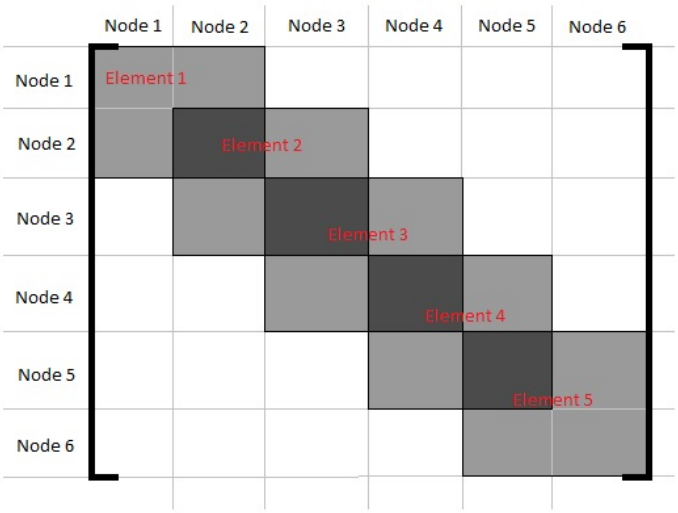

Figure 6: Assembling Global Rotor Matrices

where

$$\bar{fr}A = \frac{6I_d}{5A(1+\Phi)^2L^2}$$

$$\bar{fr}B = (\frac{1}{10} - \frac{1}{2}\Phi)\frac{I_d}{A(1+\Phi)^2L}$$

$$\bar{fr}C = (\frac{2}{15} + \frac{1}{6}\Phi + \frac{1}{3}\Phi^2)\frac{I_d}{A(1+\Phi)^2}$$

$$\bar{fr}D = -(\frac{1}{30} + \frac{1}{6}\Phi - \frac{1}{6}\Phi^2)\frac{I_d}{A(1+\Phi)^2L}.$$

Internal damping of the rotor is ignored so the element damping matrix is a twelve by twelve matrix of zeros. Then the rotor elemental matrices are combined to form global rotor matrices. This process is illustrated in Figure 6.

This process is repeated for each rotor included in the model and the global rotor matrices are assembled into the global system matrices, as illustrated in Figure 7

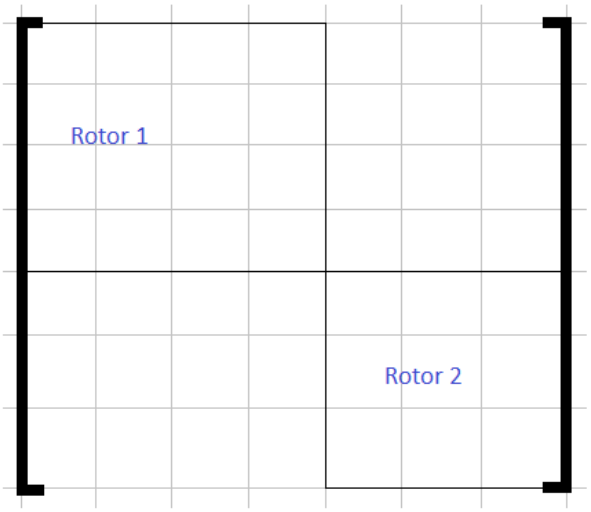

Figure 7: Assembling Global System Matrices

2.6 Rotor Components

Once the rotor model is developed, the contributions of the various rotor components can be added to the model. The following is a list of the components whose contributions to rotor systems has been examined.

- Disks
- Solid Geometry Bearings
- Tilting Pad Bearings
- Flexible Bearing Supports
- Thrust Bearings
- Aerodynamic Cross Coupling
- Linear Coupling

The inclusion of these components to the rotor model, allows the model to accurately represent many rotor systems that exist.

2.6.1 Disks

Disks can represent impellers, sleeves, fan blades, etc. Depending on the physical setup of the system, the disk will contribute significant mass and

sometimes significant stiffness to the rotor system. Disks contribute a mass of:

$$[M]^{(disk)} = \begin{bmatrix} m & 0 & 0 & 0 & 0 & 0 \\ 0 & m & 0 & 0 & 0 & 0 \\ 0 & 0 & m & 0 & 0 & 0 \\ 0 & 0 & 0 & I_p & 0 & 0 \\ 0 & 0 & 0 & 0 & I_d & 0 \\ 0 & 0 & 0 & 0 & 0 & I_d \end{bmatrix}$$

and gyroscopics of:

$$[G]^{(disk)} = \begin{bmatrix} 0 & 0 & 0 & 0 & 0 & 0 \\ 0 & 0 & 0 & 0 & 0 & 0 \\ 0 & 0 & 0 & 0 & 0 & 0 \\ 0 & 0 & 0 & 0 & 0 & 0 \\ 0 & 0 & 0 & 0 & 0 & I_p \\ 0 & 0 & 0 & 0 & -I_p & 0 \end{bmatrix}$$

to the system.

These matrices can then be added to the appropriate location in the global mass and gyroscopic matrices, respectively. If a disk is defined solely by its geometric and stiffness properties, the mass and the moments of inertia are calculated from the geometric properties of the disk using the following equations:

$$m = \rho L \pi (\frac{\phi_o^2 - \phi_i^2}{4}) \tag{2.34}$$

$$I_p = \frac{1}{2} m (\frac{\phi_o^2 + \phi_i^2}{4}) \tag{2.35}$$

$$I_d = \frac{1}{12} m [3(\frac{\phi_o^2 + \phi_i^2}{4}) + L^2] \tag{2.36}$$

If the disk also contributes stiffness properties to the system, then the disk will have a stiffness matrix of the form:

$$[K]^{(disk)} = \begin{bmatrix} 0 & 0 & 0 & 0 & 0 & 0 & 0 & 0 & 0 & 0 & 0 & 0 \\ 0 & 12*Constant & 0 & 0 & 0 & -fC & -12*Constant & 0 & 0 & 0 & -fC & \\ 0 & 0 & 12*Constant & 0 & fC & 0 & 0 & 0 & -12*Constant & 0 & fC & 0 \\ 0 & 0 & 0 & 0 & 0 & 0 & 0 & 0 & 0 & 0 & 0 & 0 \\ 0 & 0 & fC & 0 & fD & 0 & 0 & 0 & -fC & 0 & fE & 0 \\ 0 & -fC & 0 & 0 & 0 & fD & 0 & fC & 0 & 0 & 0 & fE \\ 0 & 0 & 0 & 0 & 0 & 0 & 0 & 0 & 0 & 0 & 0 & 0 \\ 0 & -12*Constant & 0 & 0 & 0 & fC & 12*Constant & 0 & 0 & 0 & fC & \\ 0 & 0 & -12*Constant & 0 & -fC & 0 & 0 & 0 & 12*Constant & 0 & -fC & 0 \\ 0 & 0 & 0 & 0 & 0 & 0 & 0 & 0 & 0 & 0 & 0 & 0 \\ 0 & 0 & fC & 0 & fE & 0 & 0 & 0 & -fC & 0 & fD & 0 \\ 0 & -fC & 0 & 0 & 0 & fE & 0 & fC & 0 & 0 & 0 & fD \end{bmatrix}$$

where

$$Constant = \frac{EI_d^{diff}}{(1+\Phi)L^3}$$

$$fC = -6L * Constant$$

$$fD = (4+\Phi)L^2 * Constant$$

$$fE = (2-\Phi)L^2 * Constant.$$

This stiffness equation is added to all of the appropriate elements that the disk encompasses in the stiffness matrix.

2.6.2 Fixed Geometry Bearings

The support structure is important to the dynamics of a rotor system. The bearings are usually the dominant source of damping for the system. It is also usually much cheaper and easier to alter the support structure of a rotor rather than the rotor itself. Therefore it is important to include it in the rotor model. The support structure can include such components such as fixed geometry bearings, tilting pad bearings, thrust bearings and flexible bearing supports.

Fixed geometry bearings contribute stiffness and damping to the system. In order to determine the stiffness and damping properties of a bearing, the bearing must be analyzed separately. This is usually done by solving Reynolds, energy and elasticity equations. There has been much work in using various reduced forms of these equations. Dynamic analysis of bearings requires the determination of the position and velocity derivatives of the integrated bearing pressure profile. For fixed pad bearings, this produces a set of eight stiffness and damping coefficients[16].

The stiffness and damping matrices of a fixed geometry bearing attached to ground are:

$$[K]^{fixed\,bearing} = \begin{bmatrix} 0 & 0 & 0 & 0 & 0 & 0 \\ 0 & K_{xx} & K_{xy} & 0 & 0 & 0 \\ 0 & K_{yx} & K_{yy} & 0 & 0 & 0 \\ 0 & 0 & 0 & 0 & 0 & 0 \\ 0 & 0 & 0 & 0 & 0 & 0 \\ 0 & 0 & 0 & 0 & 0 & 0 \\ 0 & 0 & 0 & 0 & 0 & 0 \end{bmatrix}$$

$$[C]^{fixed\,bearing} = \begin{bmatrix} 0 & 0 & 0 & 0 & 0 & 0 \\ 0 & C_{xx} & C_{xy} & 0 & 0 & 0 \\ 0 & C_{yx} & C_{yy} & 0 & 0 & 0 \\ 0 & 0 & 0 & 0 & 0 & 0 \\ 0 & 0 & 0 & 0 & 0 & 0 \\ 0 & 0 & 0 & 0 & 0 & 0 \\ 0 & 0 & 0 & 0 & 0 & 0 \end{bmatrix}$$

The stiffness and damping matrices of a fixed geometry bearing connecting multiple rotors are:

$$[K]^{fixed\,bearing} = \begin{bmatrix} 0 & 0 & 0 & 0 & 0 & 0 & 0 & 0 & 0 & 0 & 0 & 0 \\ 0 & K_{xx} & K_{xy} & 0 & 0 & 0 & 0 & 0 & 0 & 0 & 0 & 0 \\ 0 & K_{yx} & K_{yy} & 0 & 0 & 0 & 0 & 0 & 0 & 0 & 0 & 0 \\ 0 & 0 & 0 & 0 & 0 & 0 & 0 & 0 & 0 & 0 & 0 & 0 \\ 0 & 0 & 0 & 0 & 0 & 0 & 0 & 0 & 0 & 0 & 0 & 0 \\ 0 & 0 & 0 & 0 & 0 & 0 & 0 & 0 & 0 & 0 & 0 & 0 \\ 0 & 0 & 0 & 0 & 0 & 0 & 0 & 0 & 0 & 0 & 0 & 0 \\ 0 & 0 & 0 & 0 & 0 & 0 & 0 & K_{xx} & K_{xy} & 0 & 0 & 0 \\ 0 & 0 & 0 & 0 & 0 & 0 & 0 & K_{yx} & K_{yy} & 0 & 0 & 0 \\ 0 & 0 & 0 & 0 & 0 & 0 & 0 & 0 & 0 & 0 & 0 & 0 \\ 0 & 0 & 0 & 0 & 0 & 0 & 0 & 0 & 0 & 0 & 0 & 0 \\ 0 & 0 & 0 & 0 & 0 & 0 & 0 & 0 & 0 & 0 & 0 & 0 \end{bmatrix}$$

$$[C]^{fixed\,bearing} = \begin{bmatrix} 0 & 0 & 0 & 0 & 0 & 0 & 0 & 0 & 0 & 0 & 0 & 0 \\ 0 & C_{xx} & C_{xy} & 0 & 0 & 0 & 0 & 0 & 0 & 0 & 0 & 0 \\ 0 & C_{yx} & C_{yy} & 0 & 0 & 0 & 0 & 0 & 0 & 0 & 0 & 0 \\ 0 & 0 & 0 & 0 & 0 & 0 & 0 & 0 & 0 & 0 & 0 & 0 \\ 0 & 0 & 0 & 0 & 0 & 0 & 0 & 0 & 0 & 0 & 0 & 0 \\ 0 & 0 & 0 & 0 & 0 & 0 & 0 & 0 & 0 & 0 & 0 & 0 \\ 0 & 0 & 0 & 0 & 0 & 0 & 0 & 0 & 0 & 0 & 0 & 0 \\ 0 & 0 & 0 & 0 & 0 & 0 & 0 & C_{xx} & C_{xy} & 0 & 0 & 0 \\ 0 & 0 & 0 & 0 & 0 & 0 & 0 & C_{yx} & C_{yy} & 0 & 0 & 0 \\ 0 & 0 & 0 & 0 & 0 & 0 & 0 & 0 & 0 & 0 & 0 & 0 \\ 0 & 0 & 0 & 0 & 0 & 0 & 0 & 0 & 0 & 0 & 0 & 0 \\ 0 & 0 & 0 & 0 & 0 & 0 & 0 & 0 & 0 & 0 & 0 & 0 \end{bmatrix}$$

These matrices are added to the appropriate node(s) in the global stiffness matrix and global damping matrix.

2.6.3 Tilting Pad Bearings

For tilting pad bearings, the additional pad degrees of freedom generate a large number of stiffness and damping coefficients for consideration[16]. These coefficients can be reduced to a frequency dependent set of coefficients. These reduced coefficients can be treated just like a solid geometry bearing.

Otherwise you must account for the extra pad degrees of freedom. If the extra pad tilt degree of freedom is included in the model, then the damping and stiffness coefficients of the tilting pad bearing are:

$$[K]^{tilting\ pad\ bearing} = \begin{bmatrix} 0 & 0 & 0 & 0 & 0 & 0 & 0 & 0 & ... & 0 \\ 0 & K_{xx} & K_{xy} & 0 & 0 & 0 & K_{x\theta_1} & K_{x\theta_1} & ... & K_{x\theta_{NP}} \\ 0 & K_{yx} & K_{yy} & 0 & 0 & 0 & K_{y\theta_1} & K_{y\theta_2} & ... & K_{y\theta_{NP}} \\ 0 & 0 & 0 & 0 & 0 & 0 & 0 & 0 & ... & 0 \\ 0 & 0 & 0 & 0 & 0 & 0 & 0 & 0 & ... & 0 \\ 0 & 0 & 0 & 0 & 0 & 0 & 0 & 0 & ... & 0 \\ 0 & K_{\theta_1 x} & K_{\theta_1 y} & 0 & 0 & 0 & K_{\theta_1\theta_1} & 0 & ... & 0 \\ 0 & K_{\theta_2 x} & K_{\theta_2 y} & 0 & 0 & 0 & 0 & K_{\theta_2\theta_2} & ... & 0 \\ ... & ... & ... & ... & ... & ... & ... & ... & ... & ... \\ 0 & K_{\theta_{NP} x} & K_{\theta_{NP} y} & 0 & 0 & 0 & 0 & 0 & ... & K_{\theta_{NP}\theta_{NP}} \end{bmatrix}$$

$$[C]^{tilting\ pad\ bearing} = \begin{bmatrix} 0 & 0 & 0 & 0 & 0 & 0 & 0 & 0 & ... & 0 \\ 0 & C_{xx} & C_{xy} & 0 & 0 & 0 & C_{x\theta_1} & C_{x\theta_1} & ... & C_{x\theta_{NP}} \\ 0 & C_{yx} & C_{yy} & 0 & 0 & 0 & C_{y\theta_1} & C_{y\theta_2} & ... & C_{y\theta_{NP}} \\ 0 & 0 & 0 & 0 & 0 & 0 & 0 & 0 & ... & 0 \\ 0 & 0 & 0 & 0 & 0 & 0 & 0 & 0 & ... & 0 \\ 0 & 0 & 0 & 0 & 0 & 0 & 0 & 0 & ... & 0 \\ 0 & C_{\theta_1 x} & C_{\theta_1 y} & 0 & 0 & 0 & C_{\theta_1\theta_1} & 0 & ... & 0 \\ 0 & C_{\theta_2 x} & C_{\theta_2 y} & 0 & 0 & 0 & 0 & C_{\theta_2\theta_2} & ... & 0 \\ ... & ... & ... & ... & ... & ... & ... & ... & ... & ... \\ 0 & C_{\theta_{NP} x} & C_{\theta_{NP} y} & 0 & 0 & 0 & 0 & 0 & ... & C_{\theta_{NP}\theta_{NP}} \end{bmatrix}.$$

These matrices are added to the appropriate rotor and pad nodes in stiffness and damping matrices

2.6.4 Flexible Support

If the bearing is held by a flexible support then it also will contribute mass, stiffness and damping to the system. For each flexible support in the system, the number of degrees of freedom in the system is increased by two.

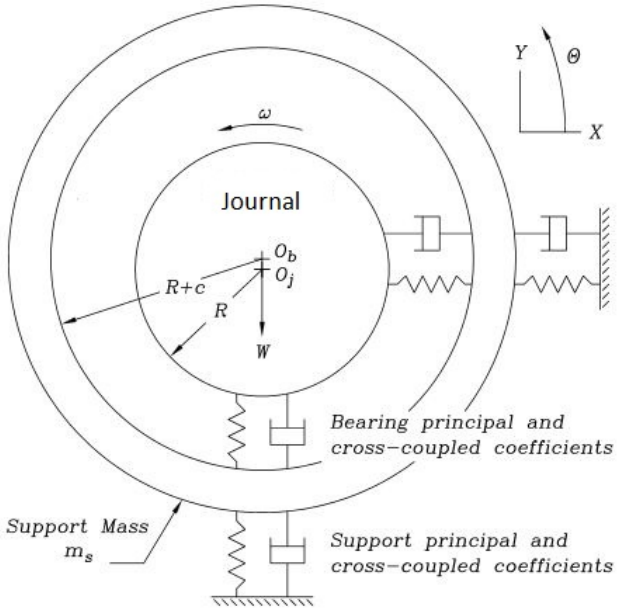

Figure 8: Fixed Geometry Bearing on a Flexible Support [17]

These two degrees of freedom are x and y displacement of the support mass. This is illustrated in Figure 8.

The stiffness and damping matrices for fixed geometry bearings held by a flexible supports are

$$[K]^{fixed\,bearing} = \begin{bmatrix} 0 & 0 & 0 & 0 & 0 & 0 & 0 & 0 \\ 0 & K_{xx} & K_{xy} & 0 & 0 & 0 & -K_{xx} & -K_{xy} \\ 0 & K_{yx} & K_{yy} & 0 & 0 & 0 & -K_{yx} & -K_{yy} \\ 0 & 0 & 0 & 0 & 0 & 0 & 0 & 0 \\ 0 & 0 & 0 & 0 & 0 & 0 & 0 & 0 \\ 0 & 0 & 0 & 0 & 0 & 0 & 0 & 0 \\ 0 & 0 & 0 & 0 & 0 & 0 & 0 & 0 \\ 0 & -K_{xx} & -K_{xy} & 0 & 0 & 0 & K_{xx} & K_{xy} \\ 0 & -K_{xy} & -K_{yy} & 0 & 0 & 0 & K_{yx} & K_{yy} \end{bmatrix}$$

$$[C]^{fixed\,bearing} = \begin{bmatrix} 0 & 0 & 0 & 0 & 0 & 0 & 0 & 0 \\ 0 & C_{xx} & C_{xy} & 0 & 0 & 0 & -C_{xx} & -C_{xy} \\ 0 & C_{yx} & C_{yy} & 0 & 0 & 0 & -C_{yx} & -C_{yy} \\ 0 & 0 & 0 & 0 & 0 & 0 & 0 & 0 \\ 0 & 0 & 0 & 0 & 0 & 0 & 0 & 0 \\ 0 & 0 & 0 & 0 & 0 & 0 & 0 & 0 \\ 0 & 0 & 0 & 0 & 0 & 0 & 0 & 0 \\ 0 & -C_{xx} & -C_{xy} & 0 & 0 & 0 & C_{xx} & C_{xy} \\ 0 & -C_{xy} & -C_{yy} & 0 & 0 & 0 & C_{yx} & C_{yy} \end{bmatrix}$$

The mass, stiffness and damping matrices for the flexible support's connection to ground are

$$[M]^{flexible\,support} = \begin{bmatrix} m_s & 0 \\ 0 & m_s \end{bmatrix}$$

$$[K]^{flexible\,support} = \begin{bmatrix} K_{xx} & K_{xy} \\ K_{yx} & K_{yy} \end{bmatrix}$$

$$[C]^{flexible\,support} = \begin{bmatrix} C_{xx} & C_{xy} \\ C_{yx} & C_{yy} \end{bmatrix}.$$

These matrices are added to the new degrees of freedom of the system.

2.6.5 Thrust Bearings

Axial loads in rotating machinery are controlled through thrust bearings[18]. Thrust bearings add axial stiffness and damping to the system similarly to the lateral bearings. Fluid film thrust bearings are analyzed in a similar manner to the lateral bearings in order to determine the eighteen stiffness and damping coefficients. Their stiffness and damping matrices are:

$$[K]^{thrust\,bearing} = \begin{bmatrix} K_{zz} & 0 & 0 & 0 & K_{z\theta_x} & K_{z\theta_y} \\ 0 & 0 & 0 & 0 & 0 & 0 \\ 0 & 0 & 0 & 0 & 0 & 0 \\ 0 & 0 & 0 & 0 & 0 & 0 \\ K_{\theta_x z} & 0 & 0 & 0 & K_{\theta_x\theta_x} & K_{\theta_x\theta_y} \\ K_{\theta_y z} & 0 & 0 & 0 & K_{\theta_y\theta_x} & K_{\theta_y\theta_y} \end{bmatrix}$$

$$[C]^{thrust\ bearing} = \begin{bmatrix} C_{zz} & 0 & 0 & 0 & C_{z\theta_x} & C_{z\theta_y} \\ 0 & 0 & 0 & 0 & 0 & 0 \\ 0 & 0 & 0 & 0 & 0 & 0 \\ 0 & 0 & 0 & 0 & 0 & 0 \\ C_{\theta_x z} & 0 & 0 & 0 & C_{\theta_x\theta_x} & C_{\theta_x\theta_y} \\ C_{\theta_y z} & 0 & 0 & 0 & C_{\theta_y\theta_x} & C_{\theta_y\theta_y} \end{bmatrix}$$

These matrices are added to the appropriate nodes in the appropriate global matrices for the rotor system.

2.6.6 Aerodynamic Cross Couplings

There are a variety of other rotor components that also have an effect on the dynamics of the rotor system. Aerodynamic cross coupling adds cross coupling stiffness to the system. This cross coupling is often a result of fluid interactions. The stiffness matrix of an aerodynamic cross coupling is

$$[K]^{cross\ coupling} = \begin{bmatrix} 0 & 0 & 0 & 0 & 0 & 0 \\ 0 & 0 & \varsigma & 0 & 0 & 0 \\ 0 & -\varsigma & 0 & 0 & 0 & 0 \\ 0 & 0 & 0 & 0 & 0 & 0 \\ 0 & 0 & 0 & 0 & 0 & 0 \\ 0 & 0 & 0 & 0 & 0 & 0 \\ 0 & 0 & 0 & 0 & 0 & 0 \end{bmatrix}$$

where ς is the magnitude of the cross coupling.

2.6.7 Rotor-to-Rotor Couplings

Many rotor systems include multiple rotors. These rotors can be connected in a variety of ways. One common way is to simply couple one end of a rotor to the end of another rotor. For many of these rotor-to-rotor couplings, they function like a linear spring between the two ends. A linear coupling has the following stiffness and damping matrices.

$$[K]^{linear\ coupling} = \begin{bmatrix}
K_{zz} & 0 & 0 & 0 & 0 & 0 & -K_{zz} & 0 & 0 & 0 & 0 & 0 \\
0 & K_{xx} & 0 & 0 & 0 & 0 & 0 & -K_{xx} & 0 & 0 & 0 & 0 \\
0 & 0 & K_{yy} & 0 & 0 & 0 & 0 & 0 & -K_{yy} & 0 & 0 & 0 \\
0 & 0 & 0 & K_{\theta_z\theta_z} & 0 & 0 & 0 & 0 & 0 & -K_{\theta_z\theta_z} & 0 & 0 \\
0 & 0 & 0 & 0 & K_{\theta_x\theta_x} & 0 & 0 & 0 & 0 & 0 & -K_{\theta_x\theta_x} & 0 \\
0 & 0 & 0 & 0 & 0 & K_{\theta_y\theta_y} & 0 & 0 & 0 & 0 & 0 & -K_{\theta_y\theta_y} \\
-K_{zz} & 0 & 0 & 0 & 0 & 0 & K_{zz} & 0 & 0 & 0 & 0 & 0 \\
0 & -K_{xx} & 0 & 0 & 0 & 0 & 0 & K_{xx} & 0 & 0 & 0 & 0 \\
0 & 0 & -K_{yy} & 0 & 0 & 0 & 0 & 0 & K_{yy} & 0 & 0 & 0 \\
0 & 0 & 0 & -K_{\theta_z\theta_z} & 0 & 0 & 0 & 0 & 0 & K_{\theta_z\theta_z} & 0 & 0 \\
0 & 0 & 0 & 0 & -K_{\theta_x\theta_x} & 0 & 0 & 0 & 0 & 0 & K_{\theta_x\theta_x} & 0 \\
0 & 0 & 0 & 0 & 0 & -K_{\theta_y\theta_y} & 0 & 0 & 0 & 0 & 0 & K_{\theta_y\theta_y}
\end{bmatrix}$$

$$[C]^{linear\ coupling} = \begin{bmatrix}
C_{zz} & 0 & 0 & 0 & 0 & 0 & -C_{zz} & 0 & 0 & 0 & 0 & 0 \\
0 & C_{xx} & 0 & 0 & 0 & 0 & 0 & -C_{xx} & 0 & 0 & 0 & 0 \\
0 & 0 & C_{yy} & 0 & 0 & 0 & 0 & 0 & -C_{yy} & 0 & 0 & 0 \\
0 & 0 & 0 & C_{\theta_z\theta_z} & 0 & 0 & 0 & 0 & 0 & -C_{\theta_z\theta_z} & 0 & 0 \\
0 & 0 & 0 & 0 & C_{\theta_x\theta_x} & 0 & 0 & 0 & 0 & 0 & -C_{\theta_x\theta_x} & 0 \\
0 & 0 & 0 & 0 & 0 & C_{\theta_y\theta_y} & 0 & 0 & 0 & 0 & 0 & -C_{\theta_y\theta_y} \\
-C_{zz} & 0 & 0 & 0 & 0 & 0 & C_{zz} & 0 & 0 & 0 & 0 & 0 \\
0 & -C_{xx} & 0 & 0 & 0 & 0 & 0 & C_{xx} & 0 & 0 & 0 & 0 \\
0 & 0 & -C_{yy} & 0 & 0 & 0 & 0 & 0 & C_{yy} & 0 & 0 & 0 \\
0 & 0 & 0 & -C_{\theta_z\theta_z} & 0 & 0 & 0 & 0 & 0 & C_{\theta_z\theta_z} & 0 & 0 \\
0 & 0 & 0 & 0 & -C_{\theta_x\theta_x} & 0 & 0 & 0 & 0 & 0 & C_{\theta_x\theta_x} & 0 \\
0 & 0 & 0 & 0 & 0 & -C_{\theta_y\theta_y} & 0 & 0 & 0 & 0 & 0 & C_{\theta_y\theta_y}
\end{bmatrix}$$

These matrices are added to the appropriate nodes on each rotor.

2.7 Equations of Motion

Equations of motion (Equations 2.14, 2.21, and 2.28) were developed for lateral, torsional, and axial directions seperately in Sections 2.1.2, 2.2.2, and 2.3.2. These equations of motion can be combined using the system matrices developed in Sections 2.5 and 2.6 to form:

$$\left[M\right]\left\{\ddot{q}\right\} + \Omega\left[G\right]\left\{\dot{q}\right\} + \left[K\right]\left\{q\right\} = \left\{F\right\} \tag{2.37}$$

In order to get direct solutions, the state space method can be used. An identity equation is added in order to form state space equation.

$$[M]\{\dot{q}\} = [M]\{\dot{q}\} \tag{2.38}$$

Equation 2.38 and Equation 2.37 can be rewritten as

$$\begin{bmatrix} 0 & M \\ M & 0 \end{bmatrix}\begin{Bmatrix}\ddot{q}\\ \dot{q}\end{Bmatrix} + \begin{bmatrix} -M & 0 \\ (C+\Omega G) & K \end{bmatrix}\begin{Bmatrix}\dot{q}\\ q\end{Bmatrix} = \begin{Bmatrix}0\\ f\end{Bmatrix}. \tag{2.39}$$

Using the change of variables

$$\{v\} = \begin{Bmatrix} \dot{q} \\ q \end{Bmatrix}, \tag{2.40}$$

Equation 2.39 can be rewritten as

$$\begin{bmatrix} 0 & M \\ M & 0 \end{bmatrix} \{\dot{v}\} + \begin{bmatrix} -M & 0 \\ (C + \Omega G) & K \end{bmatrix} \{v\} = \begin{Bmatrix} 0 \\ f \end{Bmatrix}. \tag{2.41}$$

In order to solve for the natural frequencies of the system, the force $\{f\}$ is assumed to be zero.

$$\begin{bmatrix} 0 & M \\ M & 0 \end{bmatrix} \{\dot{v}\} + \begin{bmatrix} -M & 0 \\ (C + \Omega G) & K \end{bmatrix} \{v\} = \{0\} \tag{2.42}$$

The displacement can be assumed to take the form

$$\{u(t)\} = \{U\} e^{st} \tag{2.43}$$

or

$$\{v(t)\} = \{V\} e^{st}. \tag{2.44}$$

Plugging this into Equation 2.42, yields:

$$\begin{bmatrix} 0 & M \\ M & 0 \end{bmatrix} s \{V\} e^{st} + \begin{bmatrix} -M & 0 \\ (C + \Omega G) & K \end{bmatrix} \{V\} e^{st} = \{0\} \tag{2.45}$$

or

$$\begin{bmatrix} -M & 0 \\ (C + \Omega G) & K \end{bmatrix} \{V\} = - \begin{bmatrix} 0 & M \\ M & 0 \end{bmatrix} s \{V\}. \tag{2.46}$$

We can solve for the critical speeds s and the damped mode shapes V by finding the generalized eigenvalue of these two matrices.

In order to solve for the system response to an excitation force, the force vector can not be assumed to be zero. For synchronous forces, the force vector can be assumed to be:

$$\{f\} = \{F\} e^{i\Omega t}. \tag{2.47}$$

or

$$\begin{Bmatrix} 0 \\ f \end{Bmatrix} = \begin{Bmatrix} 0 \\ F \end{Bmatrix} e^{i\Omega t} \tag{2.48}$$

Plugging this into the state space equations of motion in Equation 2.41 gives us

$$\begin{bmatrix} 0 & M \\ M & 0 \end{bmatrix} \{\dot{v}\} + \begin{bmatrix} -M & 0 \\ (C + \Omega G) & K \end{bmatrix} \{v\} = \begin{Bmatrix} 0 \\ F \end{Bmatrix} e^{i\Omega t}. \tag{2.49}$$

It is assumed that the system response will be synchronous with the running speed.

$$\{v\} = \{V\} e^{i\Omega t} \tag{2.50}$$

This gives us

$$\begin{bmatrix} 0 & M \\ M & 0 \end{bmatrix} i\Omega \{V\} e^{i\Omega t} + \begin{bmatrix} -M & 0 \\ (C + \Omega G) & K \end{bmatrix} \{V\} e^{i\Omega t} = \begin{Bmatrix} 0 \\ F \end{Bmatrix} e^{i\Omega t} \tag{2.51}$$

or

$$(i\Omega \begin{bmatrix} 0 & M \\ M & 0 \end{bmatrix} + \begin{bmatrix} -M & 0 \\ (C + \Omega G) & K \end{bmatrix}) \{V\} = \begin{Bmatrix} 0 \\ F \end{Bmatrix}. \tag{2.52}$$

So the solution can be found to be

$$\{V\} = (i\Omega \begin{bmatrix} 0 & M \\ M & 0 \end{bmatrix} + \begin{bmatrix} -M & 0 \\ (C + \Omega G) & K \end{bmatrix})^{-1} \begin{Bmatrix} 0 \\ F \end{Bmatrix}. \tag{2.53}$$

The reaction forces at the bearing can also be calculated from the displacement and velocity response at the bearing location and the bearing stiffness and damping factors.

$$F_{x@bearing} = \dot{u}_{@bearing} C_{xx(eff)} + \dot{v}_{@bearing} C_{xy(eff)} + u_{@bearing} K_{xx(eff)} + v_{@bearing} K_{xy(eff)} \tag{2.54}$$

$$F_{y@bearing} = \dot{v}_{@bearing} C_{yy(eff)} + \dot{u}_{@bearing} C_{yx(eff)} + v_{@bearing} K_{yy(eff)} + u_{@bearing} K_{yx(eff)} \tag{2.55}$$

where $C_{(eff)}$ is the effective damping, and $K_{(eff)}$ is the effective stiffness. For a bearing connected to ground this is just the damping and stiffness coefficients of the bearing. For a bearing attached to a flexible support this is:

$$C_{(eff)} = \frac{1}{\frac{1}{C_{fixed\,bearing}} + \frac{1}{C_{flexible\,support}}} \tag{2.56}$$

and

$$K_{(eff)} = \frac{1}{\frac{1}{K_{fixed\,bearing}} + \frac{1}{K_{flexible\,support}}}. \tag{2.57}$$

3 RotorSol

3.1 Overview

RotorSol is a finite element based code written in MATLAB that performs steady state rotordynamic analysis. This chapter will discuss the current capabilities of RotorSol. Only capabilities that have been verified will be included in this chapter. This chapter will also discuss the development process of RotorSol.

RotorSol was written as research platform to develop and incorporate new tools for rotordynamics within the ROMAC lab. It combines the capabilities of programs such as ROTSTB, RESP2V3, TWIST2 and FORSTAB. MATLAB was used as the platform for RotorSol for several reasons. MATLAB has powerful built-in numerical algorithms. MATLAB has the capability to handle and manipulate large complex matrices. It also has powerful visualization tools. MATLAB is also being taught at most engineering schools and has a lower learning curve than most programming languages. This will allow future students to more easily add contributions and upgrades to RotorSol. MATLAB also allows integration with its built-in Controls, Optimization and other specialized applications.

The downsides to using MATLAB as a development platform are mainly the need for a runtime environment in order to run the program and the dependence on a third party developer. Currently MATLAB's developer, MathWorks, has done an excellent job maintaining MATLAB. Also MathWorks provides a free runtime environment to run the program as a standalone executable. This allows RotorSol to be used without needing licenses from MathWorks.

3.2 Features

3.2.1 Degree of Freedom Coupling

The use of the twelve degree of freedom element as illustrated in Figure 2 allows for the coupling of the lateral, torsional and axial degrees of freedom. This means that there are seven possible degree of freedom coupling combinations. These combinations are:

- Axial
- Lateral
- Torsional

- Axial-Lateral
- Lateral-Torsional
- Axial-Torsional
- Axial-Lateral-Torsional

These different coupling combinations allow the inclusion in the model of various components such as gears and thrust bearings. The coupling caused by these components can cause mixed modes that would not be discovered in the separate analyses. These components can also cause significant force interactions across the various direction. An example of this can be found in Jason Kaplan's thesis[13]. The ability to ignore directions allows for more efficient runs and avoids flooding the user with data that may be negligible. Therefore, the ability to choose which directions to couple together is a powerful tool.

3.2.2 Multiple Rotors

Many times in industry, actual rotor systems are composed of multiple rotors connected by bearings, couplings or gears. Examples can include jet engines and drive trains. The use of the finite element method allows the analysis of systems with any number of rotors connected by a variety of components. In RotorSol these rotors can currently be coupled together by journal bearings and flexible couplings.

3.2.3 Rotor Components

RotorSol allows the modeling of many different rotor components as discussed in Section 2.6. The components that are currently included in RotorSol are:

- Disks

  The disks can be defined by their stiffness properties, their mass properties or both. If the stiffness properties of the disk are given, then the disk will contribute stiffness to the model.

- Solid Geometry Bearings

  A solid geometry bearing is defined by the eight translational stiffness and damping coefficients

- Tilting Pad Bearings

  A tilting pad bearing can be defined by either the eight translational stiffness and damping coefficients or the full bearing coefficients which will include the pad tilt degree of freedoms into the system model.

- Flexible Bearing Supports

  Flexible bearing supports are defined by the eight translational stiffness and damping coefficients, as well as a mass. They also introduce a new degree of freedom into the system.

- Thrust Bearings

  Thrust bearings are defined by nine stiffness coefficients (K_{zz}, $K_{z\theta_x}$, $K_{z\theta_y}$, $K_{\theta_x z}$, $K_{\theta_y z}$, $K_{\theta_x \theta_x}$, $K_{\theta_y \theta_y}$, $K_{\theta_x \theta_y}$, $K_{\theta_y \theta_x}$) and the corresponding damping coefficients.

- Aerodynamic Cross Coupling

  Aerodynamic cross couplings are defined by a magnitude.

- Linear Coupling

  Linear couplings are defined by the six principle stiffness and damping coefficients.

These components can accurately represent a large portion of the rotor dynamic systems that exist today, such as drive trains, compressors, pumps and jet engines. More components can be added to increase the variety of rotor systems that can be modeled by RotorSol.

3.2.4 Analyses

RotorSol can perform several different types of analyses on rotor system models. It can currently perform a stability analysis or a forced response analysis.

In addition to performing an analysis, RotorSol can output the system matrices. RotorSol will display these matrices in the System Matrices GUI shown in Figure 9. This allows the user to easily view and copy the system matrices in an excel format for external use.

RotorSol can perform a stability analysis on the rotor model. This is done by solving Equation 2.46 for the system eigenvalues and eigenvectors. The eigenvalues are the natural frequencies of the system while the corresponding eigenvectors are the corresponding mode shapes. These frequencies and mode shapes will be written in a output text file. RotorSol will also output a 3D

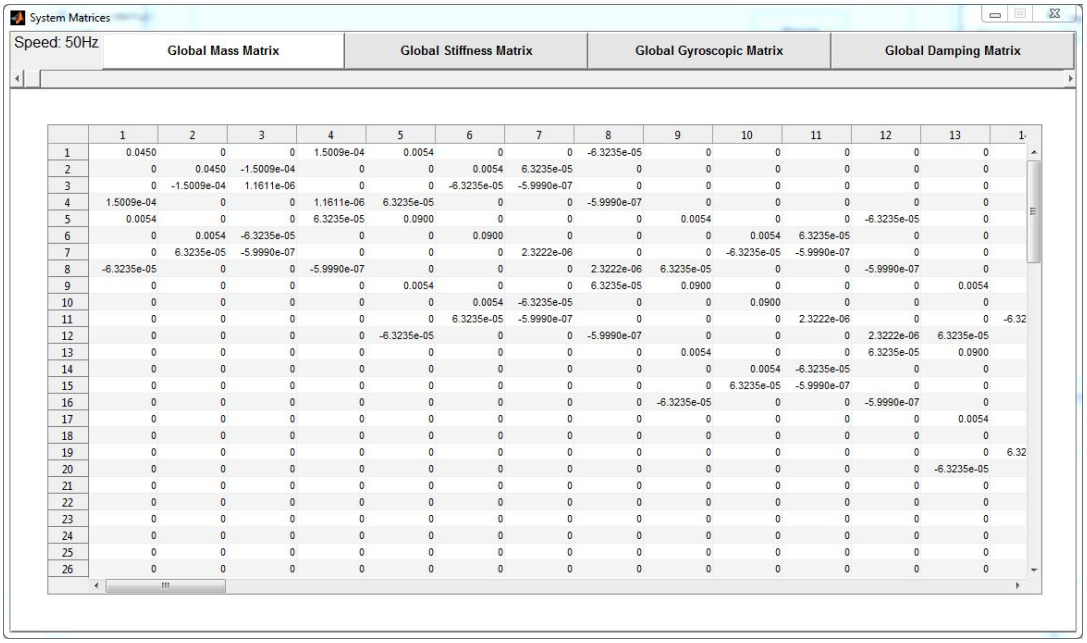

Figure 9: System Matrices GUI

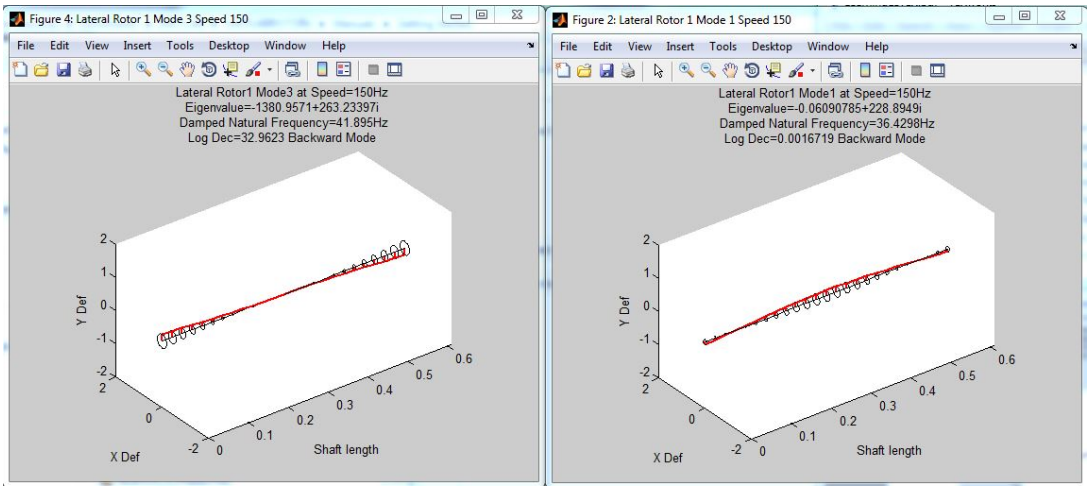

Figure 10: 3D Damped Mode Shapes

graph of the mode shapes for each natural frequency at each speed case. It will also graph a separate graph for each of the chosen direction (translational, axial and torsional) included in the analysis.

RotorSol can also perform a forced response analysis. This solves for the magnitude and phase of the rotor response assuming a steady state condition over a range of speeds. It will also solve for the reaction forces at the bearings.

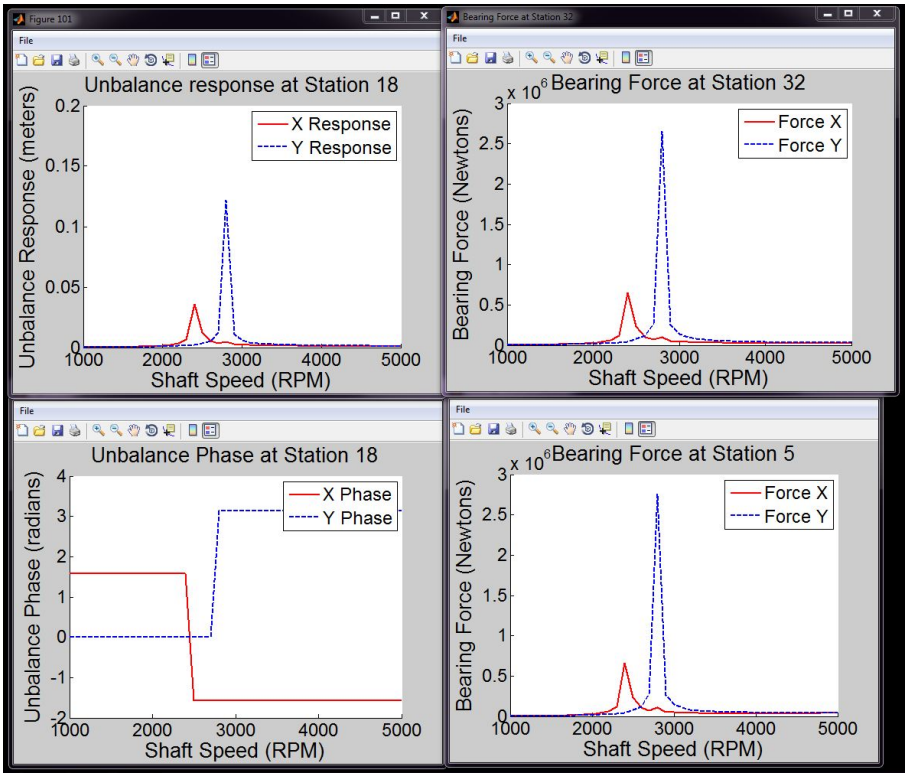

Figure 11: Probe Response Plots and Bearing Force Plots

Both probe response and bearing reaction force is graphed. The response of every node point in model is written to the output text file.

3.3 Program Efficiency

The efficiency of RotorSol has been improved greatly. These improvements vary from increases in efficiency of the code itself, changes to improve the ease of updating and adding new features, and changes to improve the interaction between RotorSol and RotorLab+, the new GUI program being developed in ROMAC that will be able to call all of the other ROMAC codes.

The development of RotorSol can be seen by examining the flow of the program through the subscripts as illustrated in Figure 12 and 13. By dividing up the content of the code into subscripts, it becomes easier to add new content and to update the existing content of RotorSol. For example, new analysis solver and post processor subscripts can be written and added easily to the appropriate places in the RotorSol and RotorSol GUI subscripts. New speed dependent components can be added easily to the Assemble Full Global System Matrices subscript, while speed independent components can

be added to the Assemble KGM Rotor Matrices subscript. Previously, the appropriate locations had to be located within the thousand lines of code in MATLABROTOR script. This is because the script contained all the code for the GUI, creating the model, running the analysis and performing the post processing.

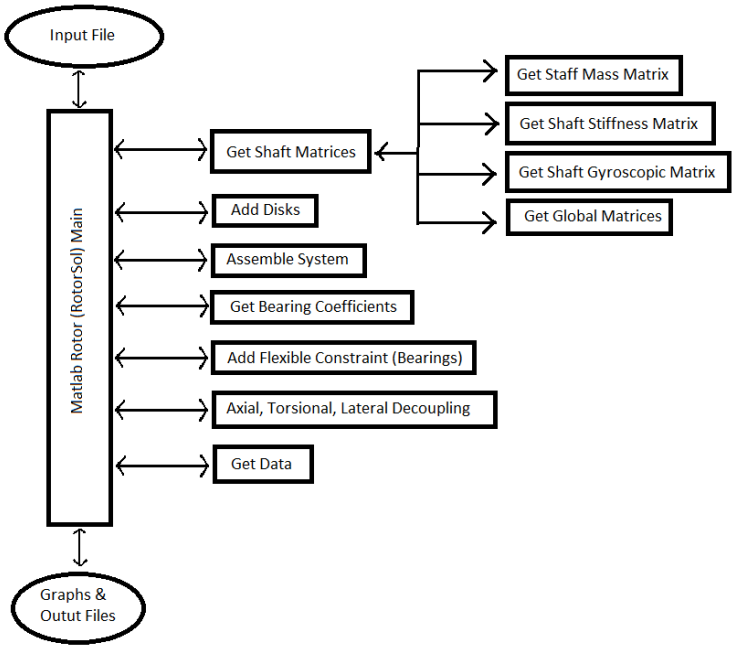

Figure 12: Initial Flowchart of MatlabRotor (RotorSol)

RotorSol's development process also allows easier communication between RotorSol and RotorLab+. RotorLab+ will be responsible for actually building the model in an excel format and for the post processing of the results. Therefore, RotorSol was broken up so that the matrix assembly and solver were in a separate batch of subscripts that could easily be compiled separately into a dll for use with RotorLab+. This branch is the RotorSol subscript and all children subscripts.

In order to improve the efficiency of the code itself, several things were done. In several places, equations were rewritten to be less computationally intensive. There were lines of code that was rewritten in order to not repeat steps needlessly and therefore improve the efficiency and run time of the code. One example of this can be seen in Figure 12 and Figure 13. The efficiency of the code was improved by breaking up the Assemble KGM Rotor Matrices and the Assemble Full Global System Matrices. Previously the entire model was created from scratch for each speed case. By breaking up these two

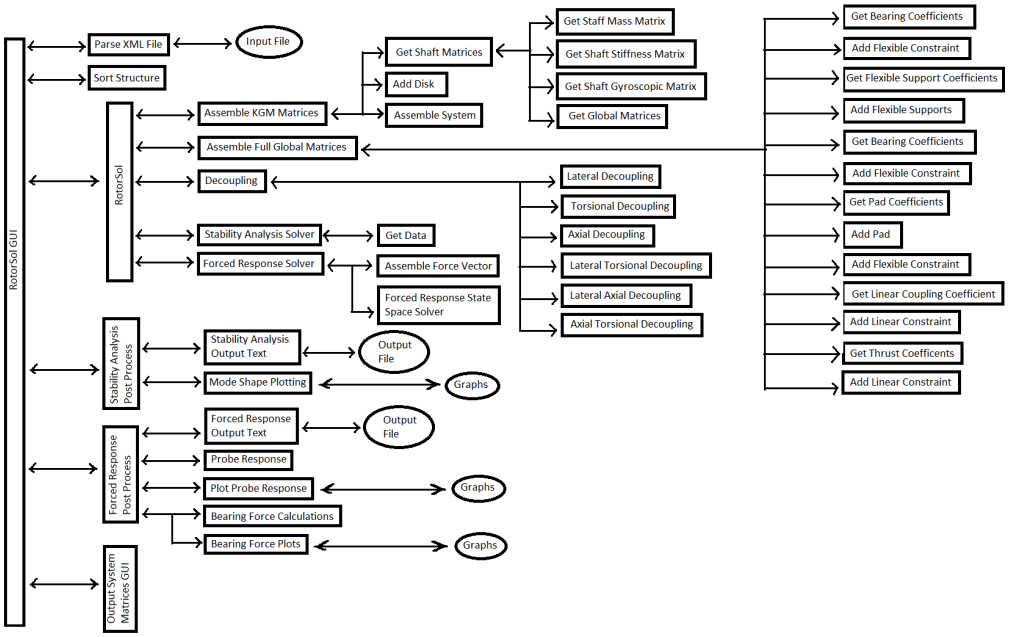

Figure 13: Current Flowchart of RotorSol

subscripts, the speed independent portion of the model is created and applied to all speeds. Then the speed dependent portion is added to the model for each speed case.

4 Verification and Validation

4.1 Overview

Verification and validation are important steps in the development of any engineering software. The engineers using the software must be confident in the results of the software in order to make intelligent decisions based on the results. It is important the the results of the software actually match up with what occurs in the real world. Verification means comparing the results of the software with other theoretical results. These can come from other validated software packages or from simple theory. Validation means comparing the results of the software with experimental data. Validation is very important as it shows direct correlation with what occurs in the field.

4.2 Eight Stage Compressor Verification

The first verification test is a model of an eight stage compressor first developed in Barrett's dissertation[19]. This compressor can be seen in Figure 14. This model is composed of thirty shaft segments(gray), two tilting pad bearings using synchronously reduced coefficients(red) and thirty disks(green). The synchronously reduced coefficients were used for the tilting pad bearings because Rotstb uses these. The model also has two probes lo-

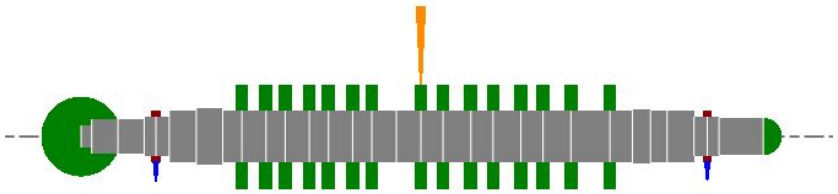

Figure 14: Eight Stage Compressor Model

cated at each of the bearings(blue) and a unbalance on the center disk(orange).

First a stability analysis was performed on this model. The rotor speed used for this analysis was five thousand rpm, and shear deformation was included in the model. The modes can be seen in Table 1. It can be seen the first ten modes have less than a 6% difference between the results from Rotstb and RotorSol. One can notice that the difference tends to increase as the mode number increases. This is caused by a difference between the transfer matrix method used by Rotstb and the finite element method used by RotorSol. The transfer matrix method tends to become more inaccurate

Mode #	Rotstb(RPM)	RotorSol(RPM)	% Difference
1	2967	2968	0.066734
2	2997	3006.288	0.30991
3	10530	10604.39	0.706439
4	10630	10705.17	0.70715
5	13800	13982.81	1.324696
6	13850	14043.58	1.397704
7	27380	27882.62	1.835734
8	27400	27896.98	1.810146
9	42180	44400.01	5.263186
10	42510	44753.46	5.277488

Table 1: First Ten Modes of the Eight Stage Compressor

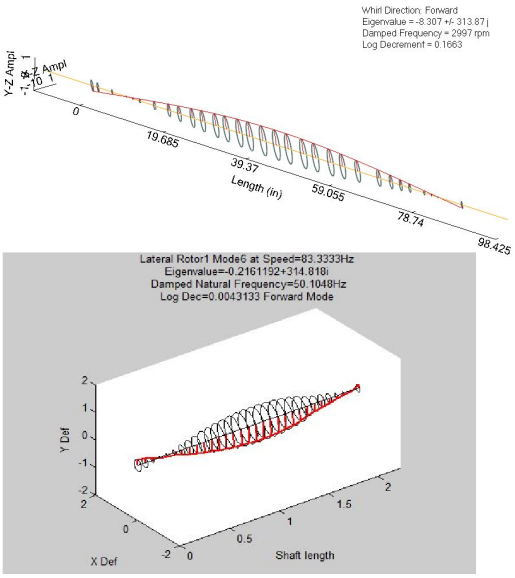

Figure 15: Mode Shapes for Mode 2

as the mode number increases. The corresponding mode shapes also match as illustrated in Figure 15 and 16.

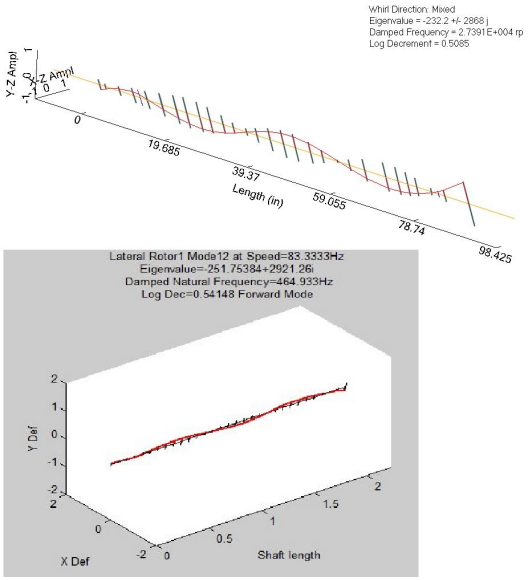

Figure 16: Mode Shapes for Mode 8

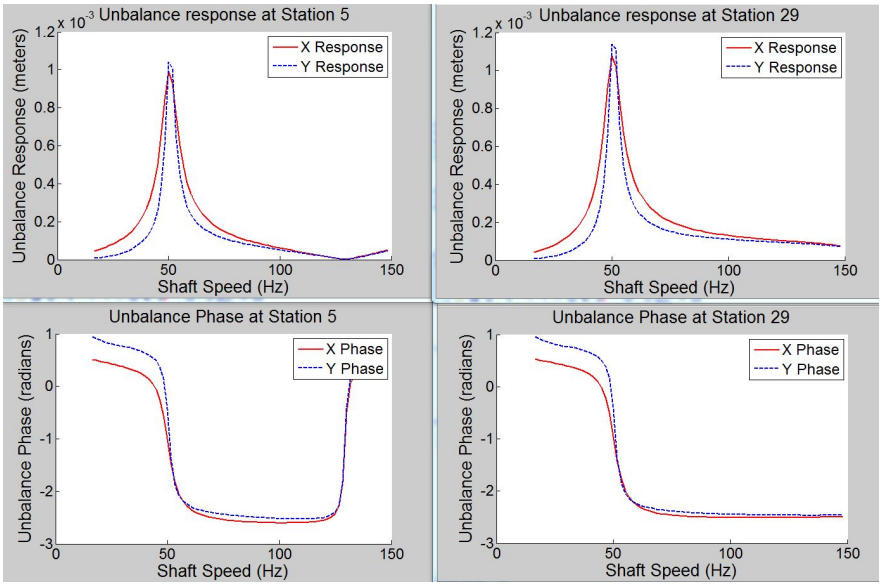

Figure 17: Probe Response Calculated by RotorSol

A forced response analysis was also performed in RotorSol and RESP2V3. In order to run this analysis probes(blue) were placed at the bearing locations and an unbalance vector(orange) was placed at the center of the shaft. Both of these components can be seen in Figure 14.

Figure 17 and Figure 18 are the graphical outputs from RotorSol and

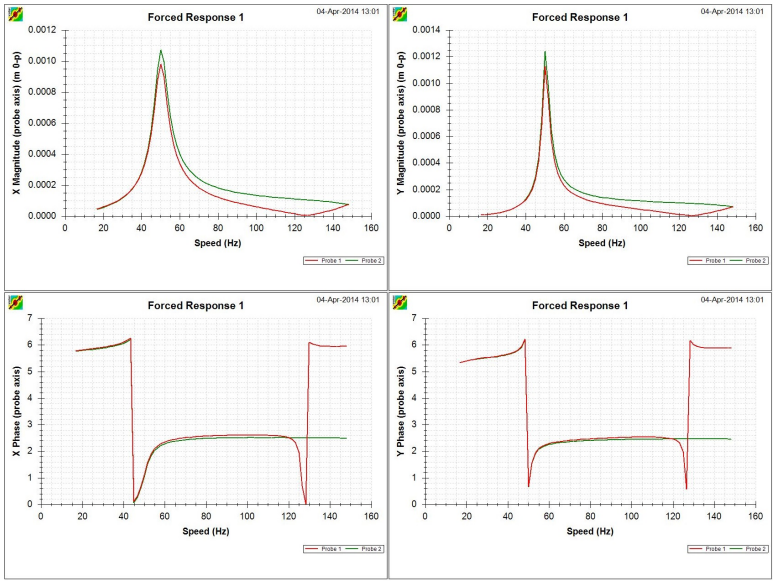

Figure 18: Probe Response Calculated by RESP2V3

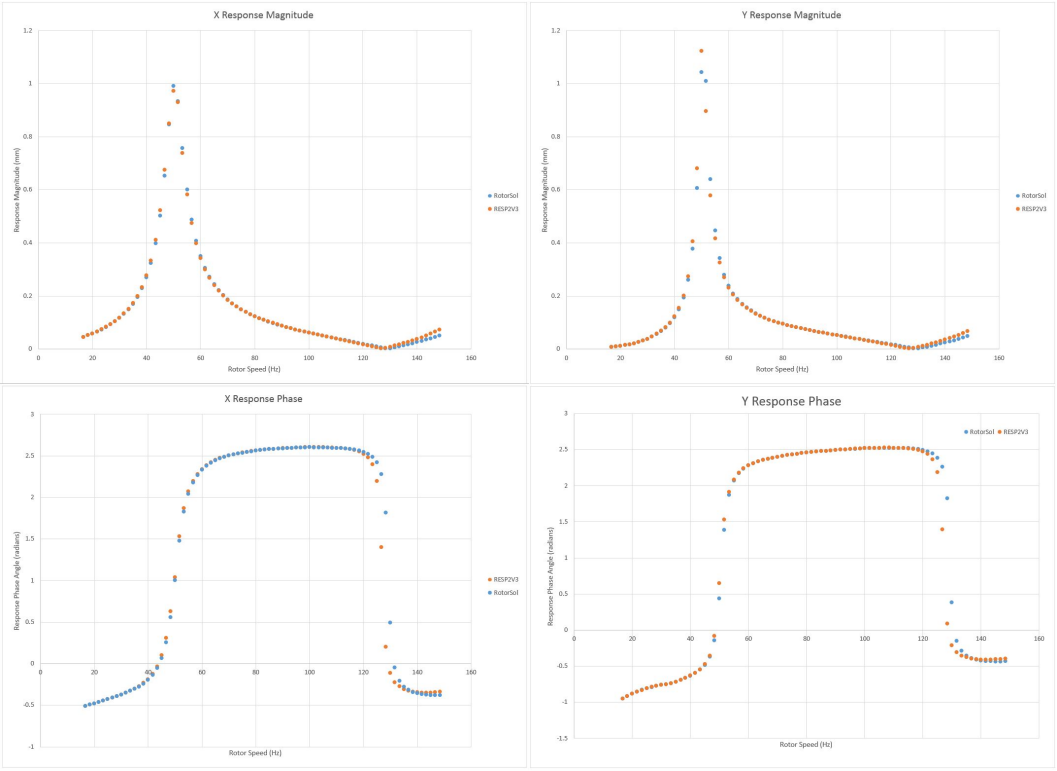

Figure 19: Comparison of Adjusted RESP2V3 and Adjusted RotorSol Values

RESP2V3. All of these plots match each other. The plots from RotorSol plot the x and y response from each probe together, while the plots from RESP2V3 plot the x responses from both probes together and the y responses from both probes together. Also there are some different assumptions used to calculate the phase between these two programs. RotorSol assumes a phase lead and calculates the phase between $-\pi$ and π. RESP2V3 assumes a phase lag and calculates the phase between 0 and 2π. Figure 19 shows the output from RotorSol adjusted to assume a phase lag and unwrapped to be a continuous curve and the output of RESP2V3 converted to metric units. Now the curves matches up with the the curves calculated by RESP2V3.

4.3 ROMAC Fluid Film Bearing Test Rig

The first validation model for RotorSol is ROMAC's Fluid Film Bearing Test Rig. RotorSol will be compared with the data found in Hunter Cloud's PhD thesis[20].The test rig is composed of a rotor with three disks on it that is supported by two tilting pad bearings. The model of this test rig consists of a single rotor composed of 63 elements. The three disks on the rotor were modeled as differences between the stiffness and mass diameters. The model using mass properties can be seen in Figure 20 while the equivalent model with stiffness properties can be seen in Figure 21.

Figure 20: Mass Properties

Figure 21: Stiffness Properties

The tilting pad bearings used in the rig can be seen in Figure 22. The dynamic properties of the bearings for use in the rotor model were determined using the thermoelastohydrodynamic algorithm, THPAD[18].

A stability analysis was performed on the test rig and was compared with Forstab, Rotstb and RotorSol. The first forward and backward bending modes were determined at eight speeds ranging from 2000 rpm to 12000

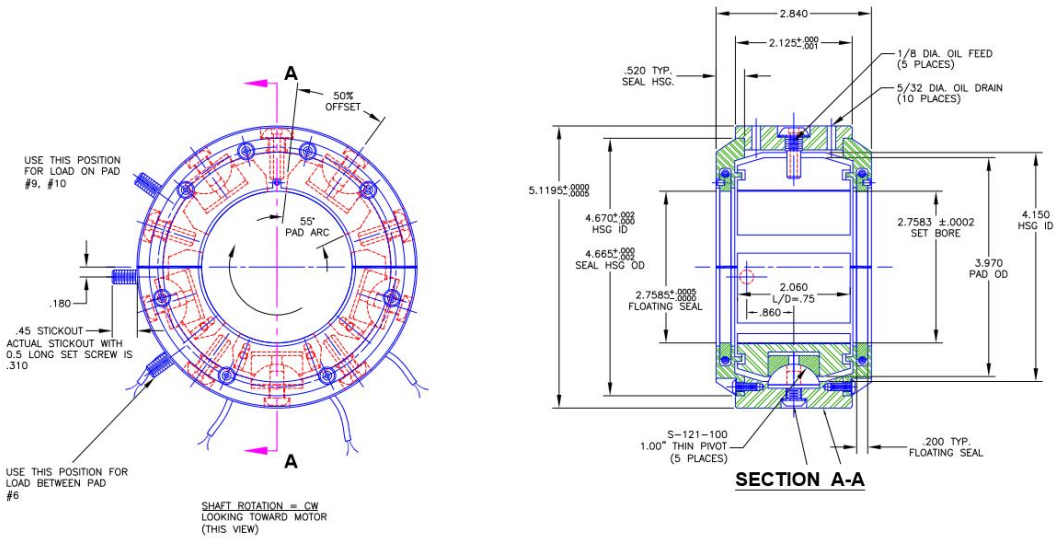

Figure 22: Tilting pad Journal Bearing Assembly (Dimensions are in inches)[20]

rpm. The analysis in RotorSol was run using both full coefficients and synchronously reduced coefficients for the tilting pad bearings. Figure 23a shows the results from the test rig compared results of the first forward bending mode with analytical results using the transfer matrix method. Figure 23b shows the results from RotorSol and ROTSTB. For the first forward mode, the biggest percent difference between the test data and RotorSol was approximately 3%. This held true for the models with both synchronously reduced coefficients and full coefficients.

Similarly, Figure 24a shows the results from the test rig compared to results of the first forward bending mode with analytical results using the transfer matrix method, while Figure 24b shows the results from RotorSol and ROTSTB. The biggest percent difference between the test data and the RotorSol model using full coefficients is approximately 1%. For the model with synchronously reduced coefficients the maximum percent difference is 4%. This shows an excellent agreement between RotorSol and the test data.

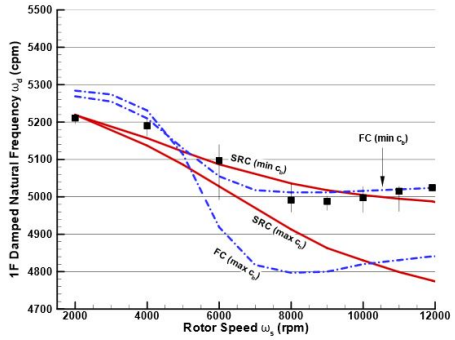

(a) Test Data and Forstab

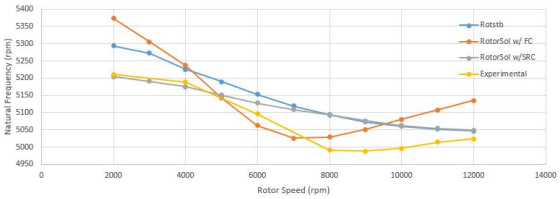

(b) RotorSol, ROTSTB and Test Data

Figure 23: First Bending Mode with Forward Whirl

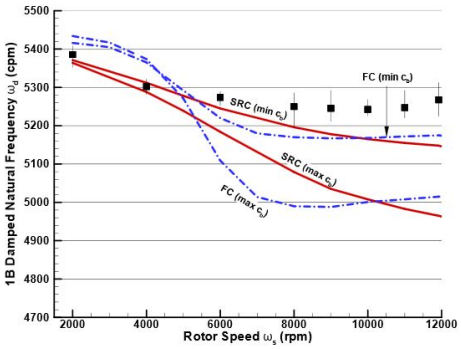

(a) Test Data and Forstab

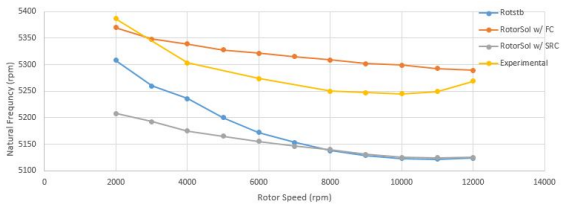

(b) RotorSol, ROTSTB and Test Data

Figure 24: First Bending Mode with Backward Whirl

5 Conclusion

The development of a variety of new features for use in a finite element approach to stability and forced response analyses is presented in this thesis. These features include the ability to chose which degrees of freedom are of importance, capability to analyze multi-rotor systems, and the ability to model tilting pad bearings, aerodynamic cross couplings, thrust bearings, flexible couplings, flexible bearing supports and the stiffness properties of disks.

In order to make use of these new features, the finite element approach to rotordynamics was developed incorporating twelve degree of freedom beam elements. Once the rotor model is developed, then additional components can be included in the model. This included disks using both stiffness and mass properties, fixed geometry bearings, tilting pad bearings, flexible supports, thrust bearings, aerodynamic cross couplings and rotor-to-rotor couplings. Then the model is solved using the state space method and the equations of motion developed in this thesis.

The methods and components developed in this thesis were verified and validated using two different rotordynamic systems. The verification model was a classic ROMAC model[19] of an eight stage compressor. This model was used to validate both the stability and forced response analyses with a model that incorporates the rotor , disks, fixed geometry bearings, probes and unbalance vectors. The stability analysis showed excellent agreement although it did have an increasing percent difference as the mode number increased. This illustrated the advantage of the finite element method over the transfer matrix method used by the verification code. The forced response analysis also showed excellent agreement.

The validation case was a model of the ROMAC Fluid Film Bearing Test Rig[20]. This model contains the rotor model with differences in the stiffness and mass diameters and tilting pad bearings using full coefficients. The stability analysis from Dr. Cloud's dissertation was compared with the results from a stability analysis of the model. This data showed excellent agreement.

The new features that have been added to the finite element approach to rotordynamics in thesis provide powerful tools for the design and troubleshooting of rotordynamic systems. The new components allow for the accurate modeling of a much wider range of rotordynamic systems. The inclusion of the degree of freedom coupling allow for inclusion of new components that introduce coupling effects on the rotor. Lastly, the efficiency of the program was improved in order to aid the engineer using it.

References

[1] Rankine, W. J. Macquorn, "On The Centrifugal Force of Rotating Shafts", *The Engineer*, 1869.

[2] Dunkerley, St., "On the Whirling and Vibration of Shafts", Phil. Trans of the Royal Soc., Vol 185, pp 279-360, 1895.

[3] F*ö*ppl, A., "Das Problem der Lavalschen Turbinenwelle", *Der Civilingenieur*, Vol 4, pp 335-342, 1895.

[4] Jeffcott, H., "The Lateral Vibration of Loaded Shafts in the Neighboorhood of a Whirling Speed-The Effect of Want of Balance", *Phil. Mag.*, Vol 37, No 6, pp 301-314,1919.

[5] Fish, Jacob and Belytchko, Ted, *A First Course in Finite Elements*, Wiley, NJ, 2007.

[6] Ruhl, R. L., "Dynamics of Distributed Parameter Rotor Systems: Transfer Matrix and Finite Element Techniques", PhD Dissertation, Cornell University, 1970.

[7] Thorkildsen, T., "Solution of a Distributed Mass and Unbalanced Rotor System Using a Consistent Mass MAtrix Approach", MSE Engineering Report, Arizona State University, 1972.

[8] Polk, S. R., "Finite Element Formulation and Solution of Flexible Rotor-Rigid Disc Systems for Natural Frequencies and Critical Whirl Speeds", MSE Engineering Report, Arizona State University, 1974.

[9] Nelson, H. D., "A Finite Rotating Shaft Element Using Timoshenko Beam Theory", *ASME Journal of Mechanical Design*, Vol. 102, pp 793-803, 1980.

[10] ROMAC, <www.virginia.edu/romac>, 2008.

[11] Chaudhry, Jawad Altaf and Sheth, Pradip, "Rotor Dynamic Analysis in Matlab Framework", Masters Thesis, University of Virginia, 2008.

[12] MathWorks, <http://www.mathworks.com/products/matlab/>

[13] Kaplan, Jason, "Gearbox Dynamics in the Modeling of Rotating Machinery", Masters Thesis, University of Virginia, 2012.

[14] Ehrich, Fredric F., *Handbook of Rotordynamics*, Krieger Publishing Company, Malabar, Florida, 1999.

[15] Allaire, Pail E., *Rotordynamics for Industrial Machines*, University of Virginia, 2008.

[16] L. Branagan and L. Barrett, "Thermal Analysis of Fixed and Tilting Pad Journal Bearings Including Cross-Film Viscosity Variations and Deformations", ROMAC, University of Virginia, June 1988.

[17] Brockett, T. and Barrett, L., "Stability of Single-Spool Rotor-Bearing Systems Including Advanced Bearing Flexible Support Models", ROMAC, University of Virginia, 1999.

[18] Brockett, T. S. and Barrett, L. E. and Allaire, P. E., "Thermoelastohydrodynamic lubrication in Thrust Bearings", ROMAC, University of Virginia, December 1994.

[19] Barrett, L. E., Stability and nonlinear response of rotor-bearing systems with squeeze film bearings, PhD dissertation, University of Virginia, 1978.

[20] C. Hunter Cloud, Eric H. Maslen, Lloyd E. Barrett, "Stability of Rotors Supported by Tilting Pad Journal Bearings", ROMAC, University of Virginia, February 2007.

[21] Genta, Giancarlo, *Dynamics of Rotating Systems*, Springer, NY, 2005.

[22] Krämer, Erwin, *Dynamics of Rotors and Foundations*, Springer-Verlag, New York, 1993.

[23] Dimond, Tim and Younan, Amir and Allaire, Paul, "The Effect of Tilting Pad Journal Bearing Dynamic Models on the Linear Stability Analysis of an 8-Stage Compressor", ROMAC, University of Virginia, September 2010.

[24] Lalanne, Michael and Ferraris, Guy, *Rotordynamics Prediction in Engineering*, 2nd Edition, John Wiley & Sons Ltd., NY, 1998.

[25] Dimond, Timothy and Younan, Amir and Sheth, Predip and Allaire, Paul, "Tilting-Pad Journal Bearing Dynamic Full Coefficient and Synchronously Reduced Properties Using Modal Analysis", ROMAC, University of Virginia, 2008.